EDL-M878

AD

(1)

TECHNICAL REPORT ECOM-00379-M878

Line-of-Sight Propagation Experimentation and Modeling for Partially Illuminated Terrain

By

H. N. GITTERMAN - S. N. WATKINS

DISTRIBUTION OF THIS DOCUMENT IS UNLIMITED

NOVEMBER 1965

ECOM

UNITED STATES ARMY ELECTRONICS COMMAND FORT MONMOUTH, N.J.

CONTRACT DA 28-043 AMC-00379(E)

SYLVANIA
ELECTRONIC DEFENSE LABORATORIES
Mountain View, California

Technical Report ECOM-00379-M878

LINE-OF-SIGHT PROPAGATION EXPERIMENTATION AND MODELING FOR PARTIALLY ILLUMINATED TERRAIN

1 November 1965

DISTRIBUTION OF THIS DOCUMENT IS UNLIMITED

This report was prepared for the Electronic Warfare Laboratory, U.S. Army Electronics Command, by the Electronic Defense Laboratories, Sylvania Corporation, under Contract DA 28-043 AMC-00379(E). Conclusions and views contained herein are those of the contractor, and are based on analysis of such information as could be made available to the contractor under terms of the contract and appropriate security directives.

Prepared by

ELECTRONIC DEFENSE LABORATORIES
SYLVANIA ELECTRIC PRODUCTS INC.
Mountain View, California 94040

For

U.S. ARMY ELECTRONICS COMMAND, FORT MONMOUTH, NEW JERSEY 07703

CONTENTS

ILLUSTRATIONS

ILLUSTRATIONS --Continued

ILLUSTRATIONS --Continued

TABLES

Section 1

ABSTRACT

A series of experiments was conducted to evaluate a model that predicts line-of-sight (LOS) propagation loss over partially illuminated terrain. Height-gain measurements were made at the receiver for a number of paths of varying irregularity, roughness, and vegetation cover. The measurements indicate that two regions must be recognized: the first, below 500 Mc, where specular effects are predominant and the specular reflection coefficient varies from approximately 0.20 to unity, and the second, above 500 Mc, where both the specular and the diffuse components must be considered and where both the specular and the diffuse reflection coefficients generally range from 0.20 to 0.40. Appropriate changes have been made in the original LOS model to reflect more accurately the propagation effects in these two regions over the frequency range of interest: 40 Mc to 20 Gc.

Section 2

INTRODUCTION

A signal-environment model was developed at EDL to predict the signal strength at a receiver located up to 15 kilometers behind the FEBA (forward edge of the battle area) when the transmitter lies anywhere within a typical tactical division. This work is reported in EDL document EDL-M768 entitled "A Computer Model for the Simulation of Tactical Signal Environments."[1] The model processes the deployment and characteristics of the transmitter, the terrain features, and possible propagation modes to determine signal strengths for frequencies within the range 40 Mc to 20 Gc. It provides a means to define, rapidly, EW (electronic warfare) systems requirements and to evaluate EW systems in a tactical signal environment.

Propagation modes were characterized under the general headings of line-of-sight (LOS) conditions and non-line-of-sight (NLOS) conditions. For those modes falling within the latter category (diffraction and tropospheric scatter), models developed at the National Bureau of Standards (NBS) were used to predict path loss. For the LOS conditions expected, no model considered suitable was available. The typical situation encountered for this mode of propagation involves very small grazing angles and only partial illumination of the reflecting surface. Most LOS models available are based on uniform illumination of the surface and involve some form of statistical description[2,3,4] of that surface and, consequently, are not applicable to this study.

An LOS model was developed and reported in EDL-768 that allows determination of the propagation loss as a function of the total power scattered by the reflecting surface. The utility of the model is that the determination of this scattered power is a relatively simple process, namely: 1) geometrical constructions to find the angle of incidence to each of the reflecting segments, 2) determination of the reflection coefficient for each segment, using experimental curves that plot the reflection coefficient

1. See list of references in Section 10.

as a function of the angle of incidence for the types of terrains encountered, and 3) summing the scattered power from each segment over all the reflecting segments.

An experimental program was designed to test the model. The results of the program are discussed in detail in this report. Eleven paths in the area, of varying irregularity, roughness, and vegetation cover, were selected for measurements of path loss. A frequency range of 100 to 10,000 Mc was chosen for this initial study. Continuous height-gain curves were plotted for each frequency-path combination to observe any reflection coefficient variations.

The major findings of this program indicate that two distinct frequency regions exit: the first, below about 500 Mc, where specular reflection is the dominant scattering mode and the second, above 500 Mc, where the scattering is a result of both specular and diffuse modes. Accordingly, appropriate revisions were made in the original theoretical model to incorporate these effects.

The automation of the LOS and NLOS models, with the necessary revisions incorporated in both the models, is discussed in EDL-M879, entitled "Automated Signal Environment Model: Revised Capabilities."[5]

Section 3

REVIEW OF INITIAL LOS MODEL FORMULATION

The field scattered by a rough surface can, in general, be considered the sum of two components: a specular component and a diffuse component. The specular component is a reflection of the same type as is caused by a smooth surface; it is directional and obeys the laws of geometrical optics. Its phase is coherent, and it is the result of the radiation of points on the Fresnel ellipses. Diffuse scattering is a phenomenon that has little directivity and consequently takes place over a much larger area than the first Fresnel zone. Its phase is incoherent. Because the terrain encountered in this study generally had extensive vegetation growth (grass and trees), normally resulting in a greatly diminished specular component, a major assumption in the model was

a. diffuse reflection is the predominant mode of scattering, with specular reflection providing only a second-order effect.

Two other important assumptions were made. These were

b. for the frequency range 40-20,000 Mc, the reflection coefficient is frequency independent, and

c. for a given angle of incidence, the reflection coefficient is constant for terrain up to 125 meters in extent.

The portions of the surface capable of supporting direct reflection from transmitter to receiver were found and divided into segments up to 125 meters, and the angle of incidence from the transmitter to each segment was determined. From experimental curves of Sherwood and Ginzton,[6] the reflection coefficient was found as a function of angle of incidence, terrain cover, and polarization.

3. --Continued

The total scattered field at the receiver, due to the segments, is

$$E_s = \sum_{k=1}^{m} E_k \rho_k e^{j\varphi_k}, \tag{1}$$

where

m = the number of segments,

E_k = the amplitude of the wave incident on the k^{th} segment,

ρ_k = the magnitude of the reflection coefficient from the k^{th} segment, and

φ_k = the phase of the reflection coefficient from the k^{th} segment, given by

$$\varphi_k = \frac{2\pi}{\lambda} \Delta r_k + \pi,$$

where λ is the wavelength and Δr_k is the path length difference between direct and reflected wave.

With diffuse scattering predominant, the phase of the reflected wave from any segment, k, can take on any value in the range $-\pi$ to π with equal probability. The φ_k are uniformly distributed, and the resultant scattered field amplitude, E_s, takes on a Rayleigh distribution.

If X and Y are the quadrature components of E_s, their variance may be written

$$D\{x\} = \frac{1}{2} \sum_{k=1}^{m} \rho_k^2 E_k^2 \tag{2}$$

$$D\{y\} = \frac{1}{2} \sum_{k=1}^{m} \rho_k^2 E_k^2 . \tag{3}$$

3. --Continued

Rice[7] studied the distribution of a constant vector and a Rayleigh vector with variance as given above. In terms of

$$E_1^2 = \sum_{k=1}^{m} \rho_k^2 E_k^2 ,$$

he found the probability distribution of the amplitude of the resultant field at the receiver to be

$$P(E) = \frac{2E}{E_1^2} \exp\left[-\frac{\left(E^2 + E_o^2\right)}{E_1^2}\right] I_o\left(\frac{2E_o E}{E_1^2}\right), \tag{4}$$

where

E = the amplitude of the resultant field

E_o = the amplitude of the direct wave and

$I_o\left(\frac{2E_o E}{E_1^2}\right)$ = a modified Bessel function, expressed as

$$I_o(x) = J_o(jx) = \frac{1}{\pi}\int_o^{\pi} \exp(x \cos\theta)\, d\theta .$$

The probability that the resultant amplitude exceeds some value, E, is

$$P\left[E' > E\right] = \int_E^{\infty} \frac{2E}{E_1^2} \exp\left[-\frac{\left(E^2 + E_o^2\right)}{E_1^2}\right] I_o\left(\frac{2E_o E}{E_1^2}\right) dE . \tag{5}$$

3. --Continued

Equation (5) has been solved by Norton, Vogler et al.[8] for R, the resultant amplitude (in db) relative to E_o .

$$R = 20 \log_{10}\left(\frac{E}{E_o}\right) \tag{6}$$

For the probabilities $P\left[E' > E\right] = 0.1, 0.5, 0.9$ and with $K = E_1/E_o$, the resultant amplitude above the constant component for $k = 20 \log_{10}\left(\frac{E_1}{E_o}\right) \geq 0$, is

$$R(0.1) = K + 3.6 + 4.34/k^2 - 2.50/k^4 + \ldots \tag{7}$$

$$R(0.5) = K - 1.6 + 4.34/k^2 - 0.752/k^4 + \ldots \tag{8}$$

$$R(0.9) = K - 9.8 + 4.34/k^2 - 0.114/k^4 + \ldots \tag{9}$$

and for $k = 20 \log_{10}\left(\frac{E_1}{E_o}\right) < 0$ is

$$R(0.1) = 7.87\ k - 1.39\ k^2 - 0.797\ k^3 + \ldots \tag{10}$$

$$R(0.5) = 2.17\ k^2 - 0.362\ k^4 + \ldots \tag{11}$$

$$R(0.9) = 7.87\ k - 1.39\ k^2 + 0.797\ k^3 + \ldots \tag{12}$$

The resultant amplitude above the constant component is then subtracted from the basic transmission loss, L_B, to find the LOS propagation path loss, L:

$$L(P) = L_B - R(P). \tag{13}$$

The basic transmission loss (in db) is

$$L_B = 10 \log \left(\frac{4\pi d}{\lambda}\right)^2, \tag{14}$$

where d is antenna separation and λ is free-space wavelength. Substituting the values for the constants, L_B becomes (expressed in db)

$$L_B = 36.6 + 20 \log_{10} d_{mi} + 20 \log_{10} f_{mc}, \tag{15}$$

3. --Continued

where

d_{mi} = antenna separation in miles

f_{mc} = frequency in megacycles.

The L_B in Equation (15) represents the signal loss between any two isotropic sources. Where directional antennas are used, their respective gain along the path in question must be subtracted from the basic loss. This new loss value, as derived in Equation (16), represents the "effective" or "apparent" loss.

$$L_{eff} = 10 \log \left(\frac{4\pi d}{\lambda}\right)^2 - G_T - G_R + D$$

$$= L_B - G_T - G_R + D$$

$$= 36.6 + 20 \log_{10} d_{mi} + 20 \log_{10} f_{mc} - G_T - G_R + D, \qquad (16)$$

where

L_{eff} = effective RF loss

L_B = basic transmission loss

G_T = gain of the transmitting antenna along the path in question

G_R = gain of the receiving antenna along the path in question

D = combined cable, mismatch, and reflector losses where these are known.

The procedure for determining the LOS propagation loss, then, is as follows.

1. Compute the amplitude of the field at the receiving antenna due to the direct ray.
2. Determine the reflection segments.
3. Compute the angle of incidence to each segment.

3. --Continued

4. Determine the reflection coefficient from the empirical reflection coefficient curves.

5. Compute the amplitude of the field reflected from each segment, and then the power.

6. Sum the reflected powers.

7. Compute the desired R(0.1), R(0.5), or R(0.9) from Equations (7), (8), and (9) or Equations (10). (11), and (12).

8. Subtract R(P) from L_{eff} to find the LOS propagation loss, L(P).

Section 4

EXPERIMENTAL PROGRAM

To test the applicability of the LOS model, a series of propagation loss measurements were made over paths in the San Francisco Bay area at 120, 350, 750, 1000, 3000, 7500, and 10,000 Mc. Eleven different paths were selected, ranging from 15,400 to 40,100 feet. Six of the paths (1, 1A, 2, 3, 4, 5) had a dense vegetation covering in the form of shrubs and trees; three paths (6, 7, 8) had a sparse vegetation covering with grass and a few trees; and two paths (9 and 10) were practically vegetation-free. Paths 1 through 8 were rough, with only portions of the surface illuminated by the transmitted signal; paths 9 and 10 were essentially flat and were added to provide comparative results, as complete surface illumination was possible. Elevation-versus-length plots for the paths are shown in Figures 1a through 1j, and path data are given in Table 1.

For paths 1 through 6 (1, 1A, 2, 3, 4, 5, 6), four sets of measurements were made for each path: two with the transmitting antenna elevated 20 feet above the ground and two with the transmitting antenna 10 feet above the ground (Figure 2). For paths 7 through 10, three sets of measurements were made: two with the transmitting antenna at 20 feet, one with the transmitting antenna at 10 feet. In each case, the receiving antenna was mounted on a 24-foot mast allowing continuous recording of the received field from 10 to 34 feet above the ground (Figure 3). A synchro sensor was attached to the motor driving the receiver antenna platform, and the output of both the sensor and the receiver IF was fed into a rectangular antenna pattern recorder to provide a height-gain curve over the 24-foot run (Figure 4). At the end of each run, the receiving mixer, which was attached directly to the receiving antenna, was connected to a calibrated signal source tuned to the measured frequency. The calibrated signal level was then adjusted to some level on the measured height-gain curve, which was then marked on the recorder chart so the magnitude of the received signal could be read directly from the chart in dbm (decibels with respect to one milliwatt). For each curve, the maximum, minimum, and mean signal loss values were determined. The resultant loss (or gain) with respect to free-space loss was then calculated. A typical data sheet is shown in Figure 5.

Table 1. Path Identification Parameters.

Path	Site		Height (feet)		Distance (feet)	Lowest Alt. (feet)	Elev. Diff. Xmit to Rec. (feet)
	From	To	From	To			
1	Bielawski Mtn.	Road Site 1	3200	2400	18,000	1.320	800
1A	Bielawski Mtn.	Hilltop	3200	2550	16,000	1,640	650
2	Bielawski Mtn.	Road Site 2	3200	1600	15,400	920	1,600
3	Bielawski Mtn.	Boulder Creek Water Tank	3200	900	33,000	640	2,300
4	Bielawski Mtn.	Eagle Rock	3200	2400	40,100	600	800
5	Boulder Creek Water Tank	Eagle Rock	900	2400	22,600	500	1,500
6	Mt. Hamilton	KREP "A" Frame	4200	2000	31,600	1,500	2,200
7	Mt. Hamilton	Quimby Road	4200	2300	27,000	1,500	1,900
8	Mt. Hamilton	Oak Ridge	4200	2400	17,500	1,900	1,800
9	County Communic. Center	Babb Creek	400	750	36,600	100	350
10	County Communic. Center	Klein Road	400	420	33,200	100	20

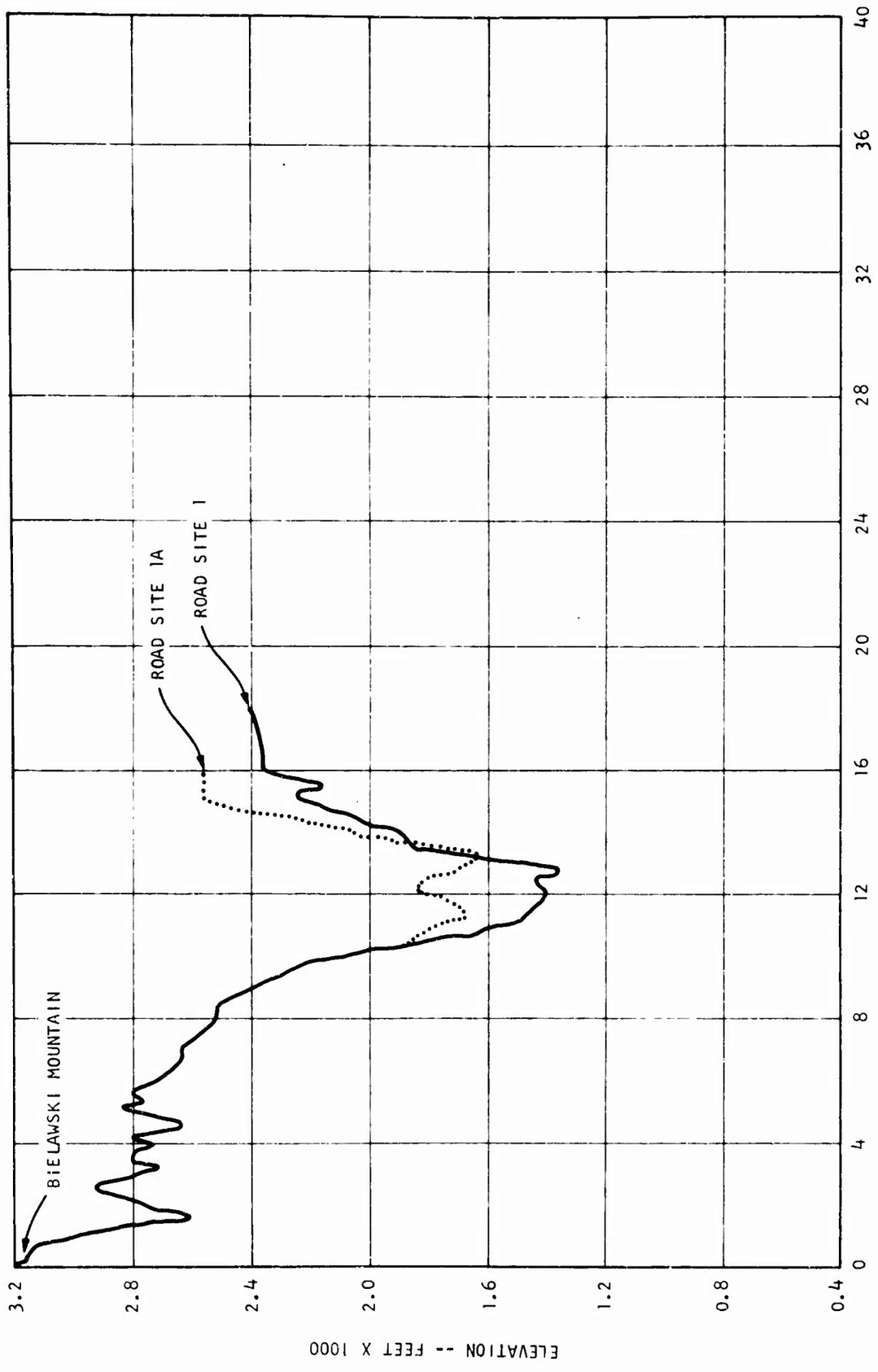

Figure 1a. Elevation Profiles, Paths 1 and 1A.

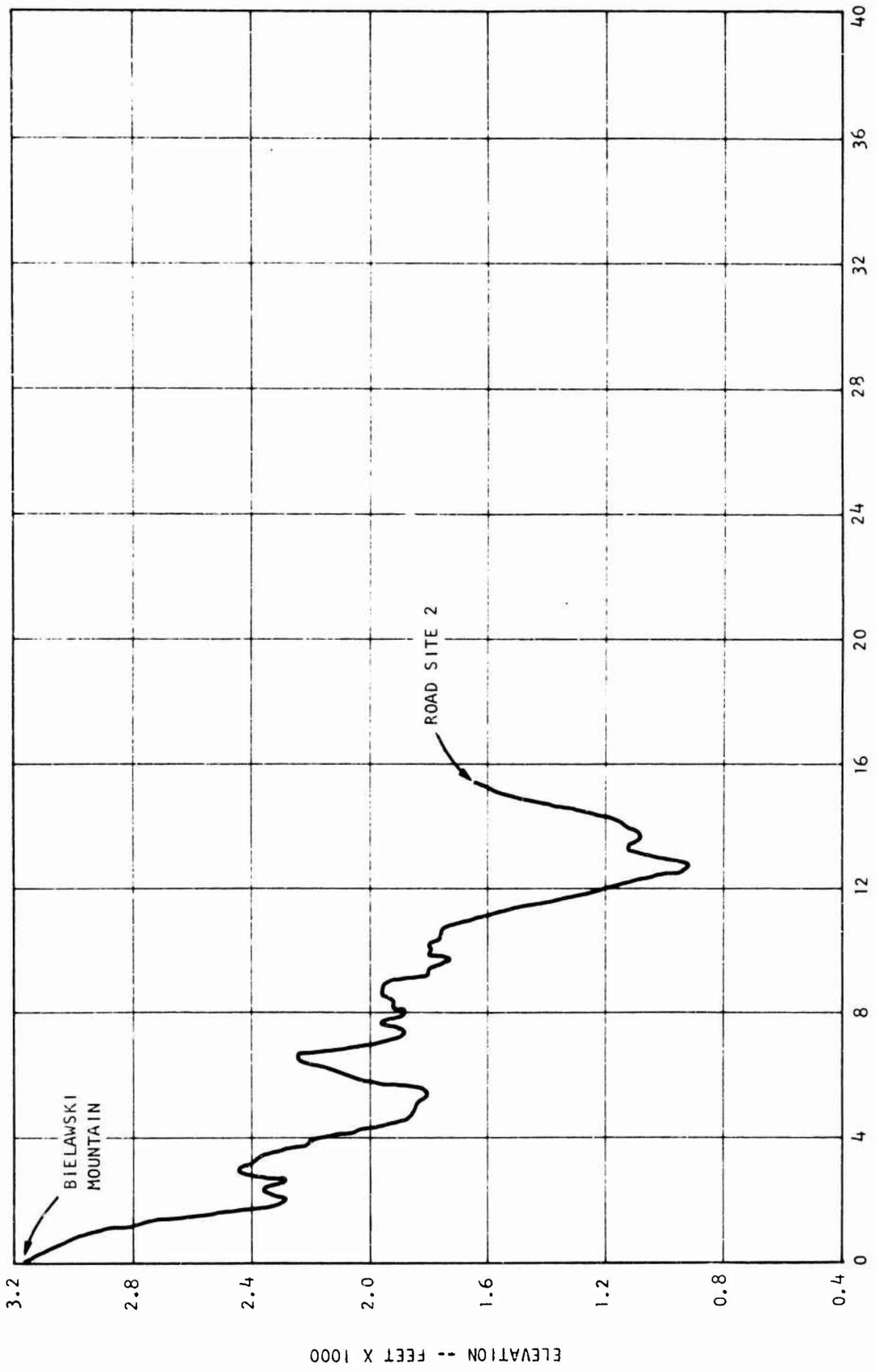

Figure 1b. Elevation Profile, Path 2.

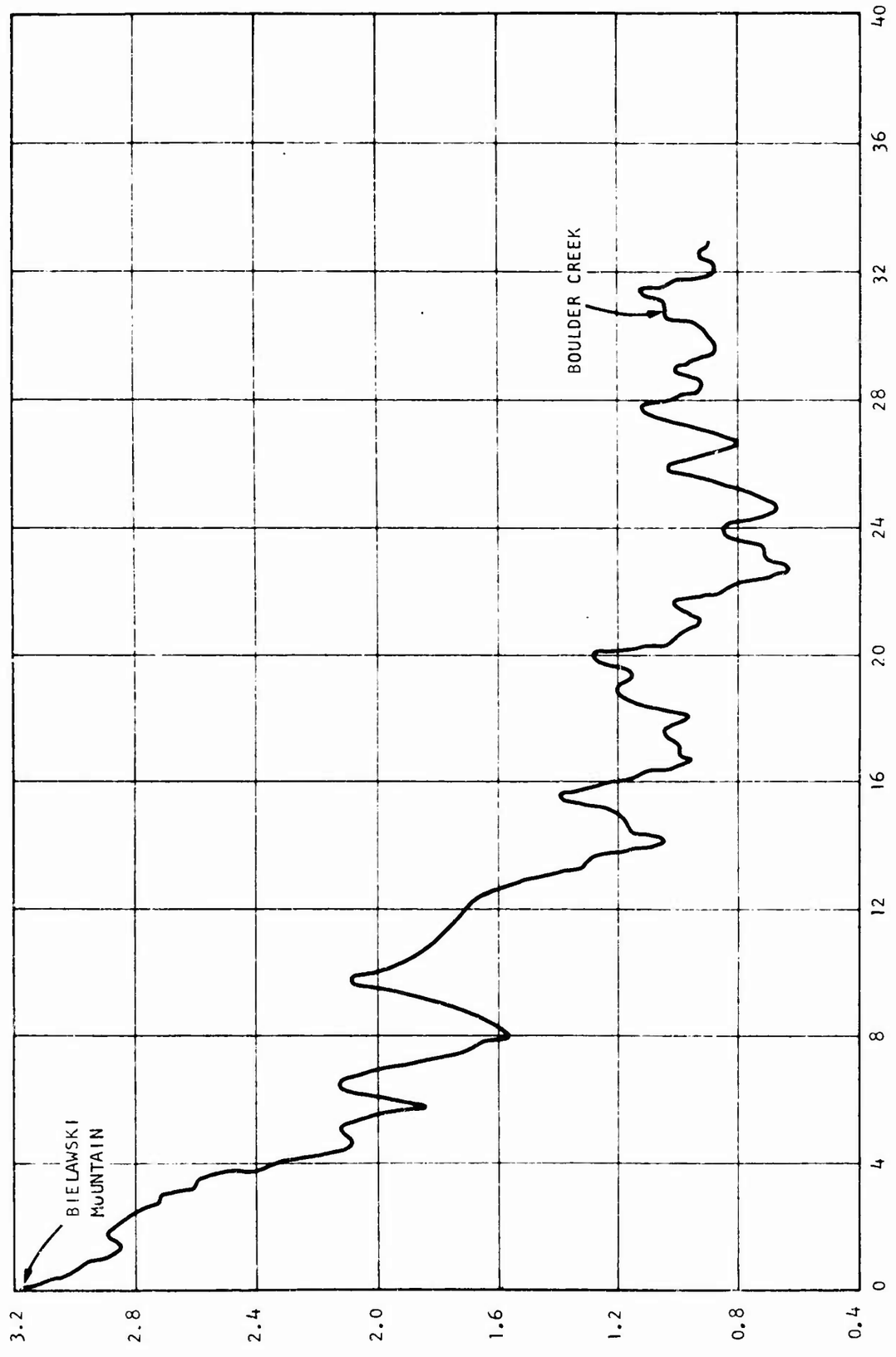

Figure 1c. Elevation Profile, Path 3.

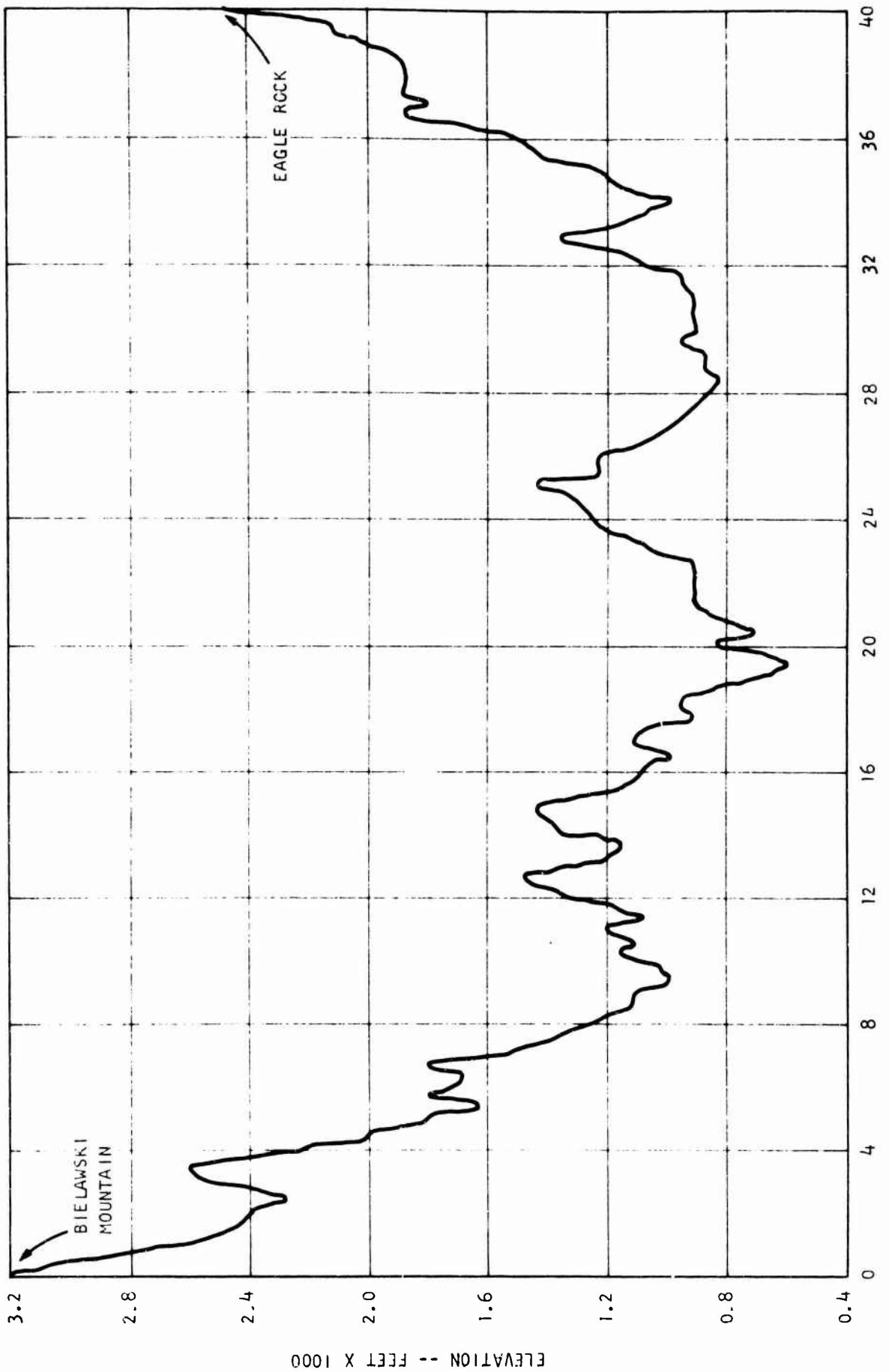

Figure 1d. Elevation Profile, Path 4.

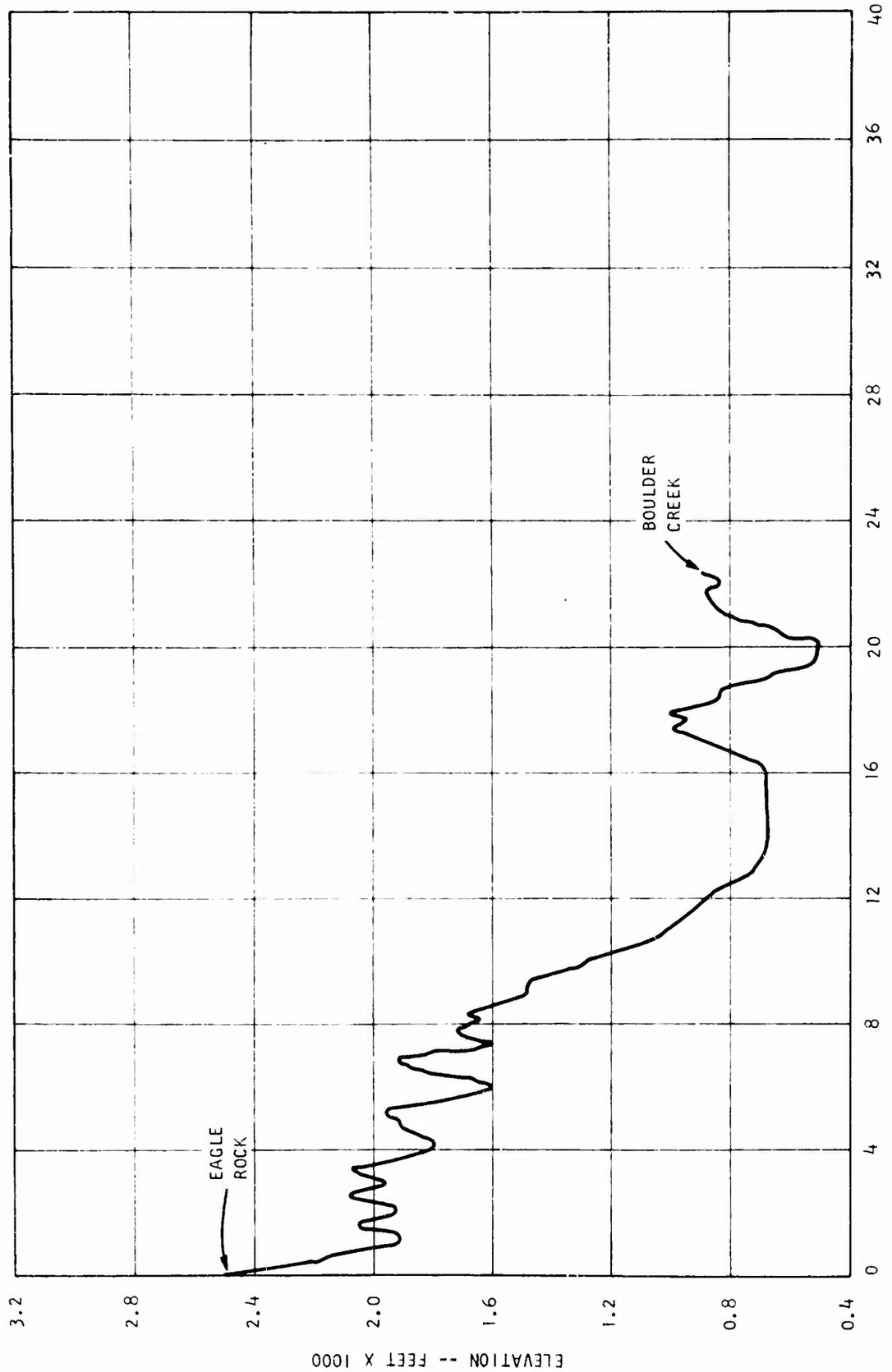

Figure 1e. Elevation Profile, Path 5.

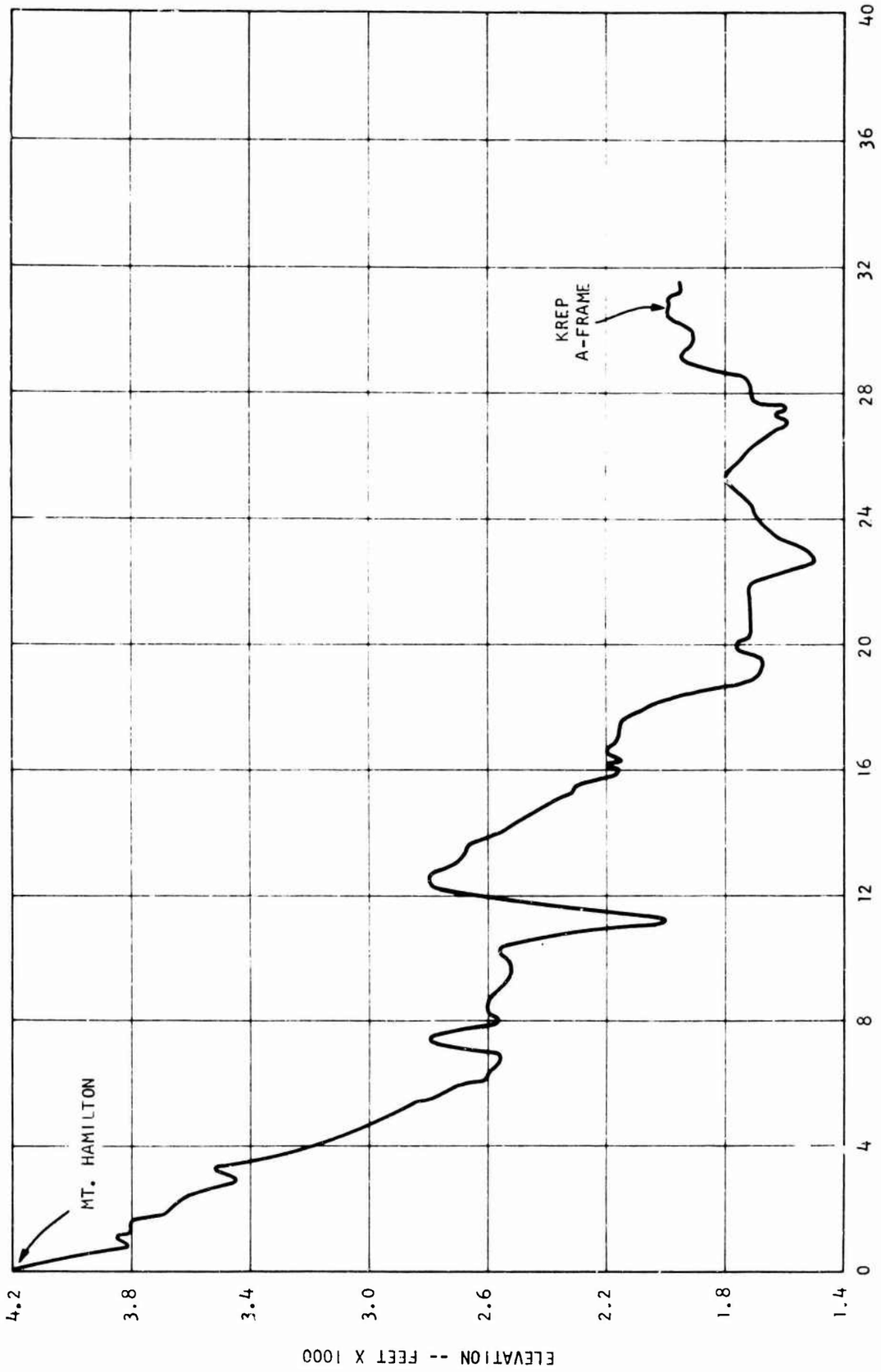

Figure 1f. Elevation Profile, Path 6.

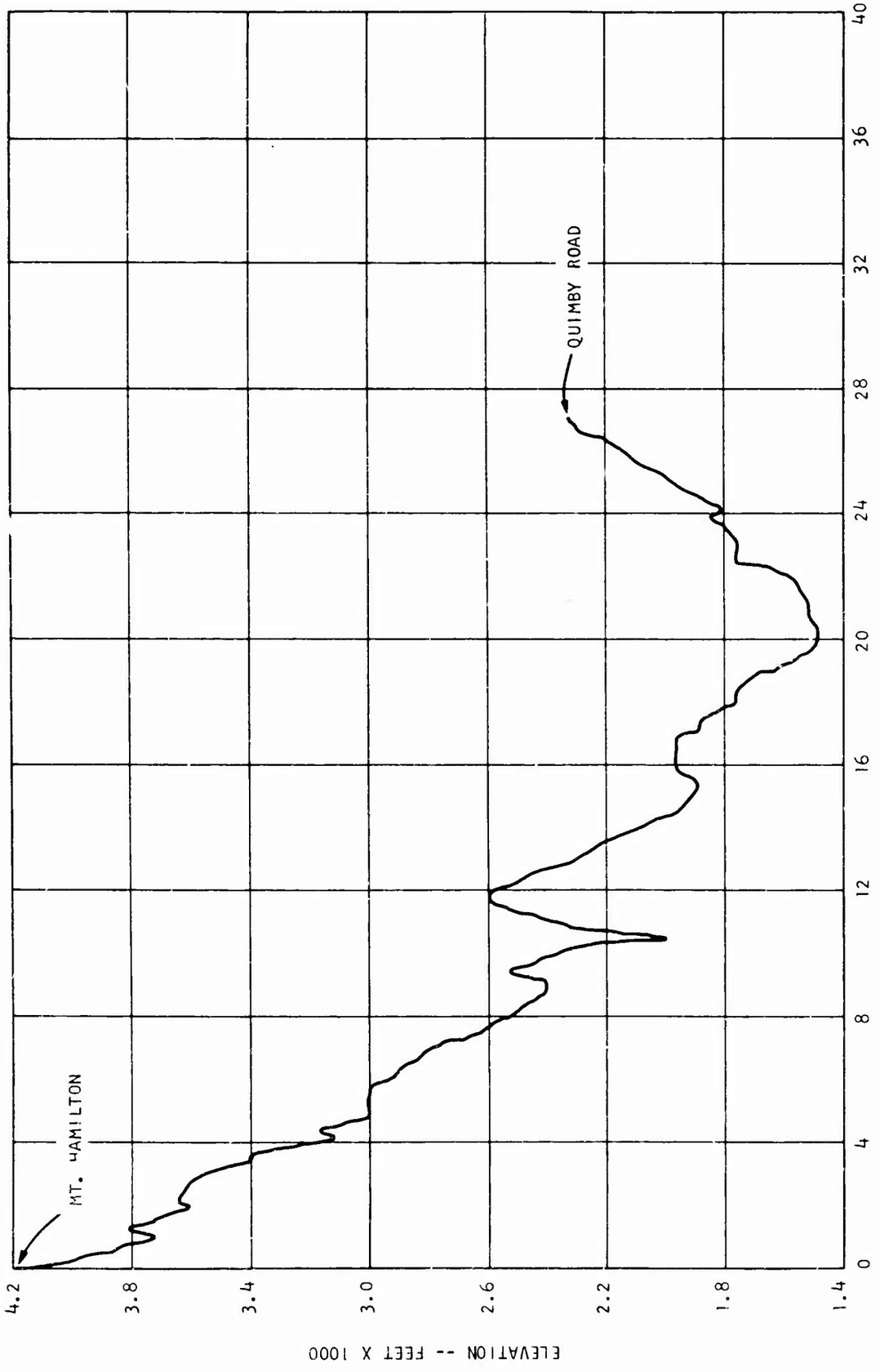

Figure 1g. Elevation Profile, Path 7.

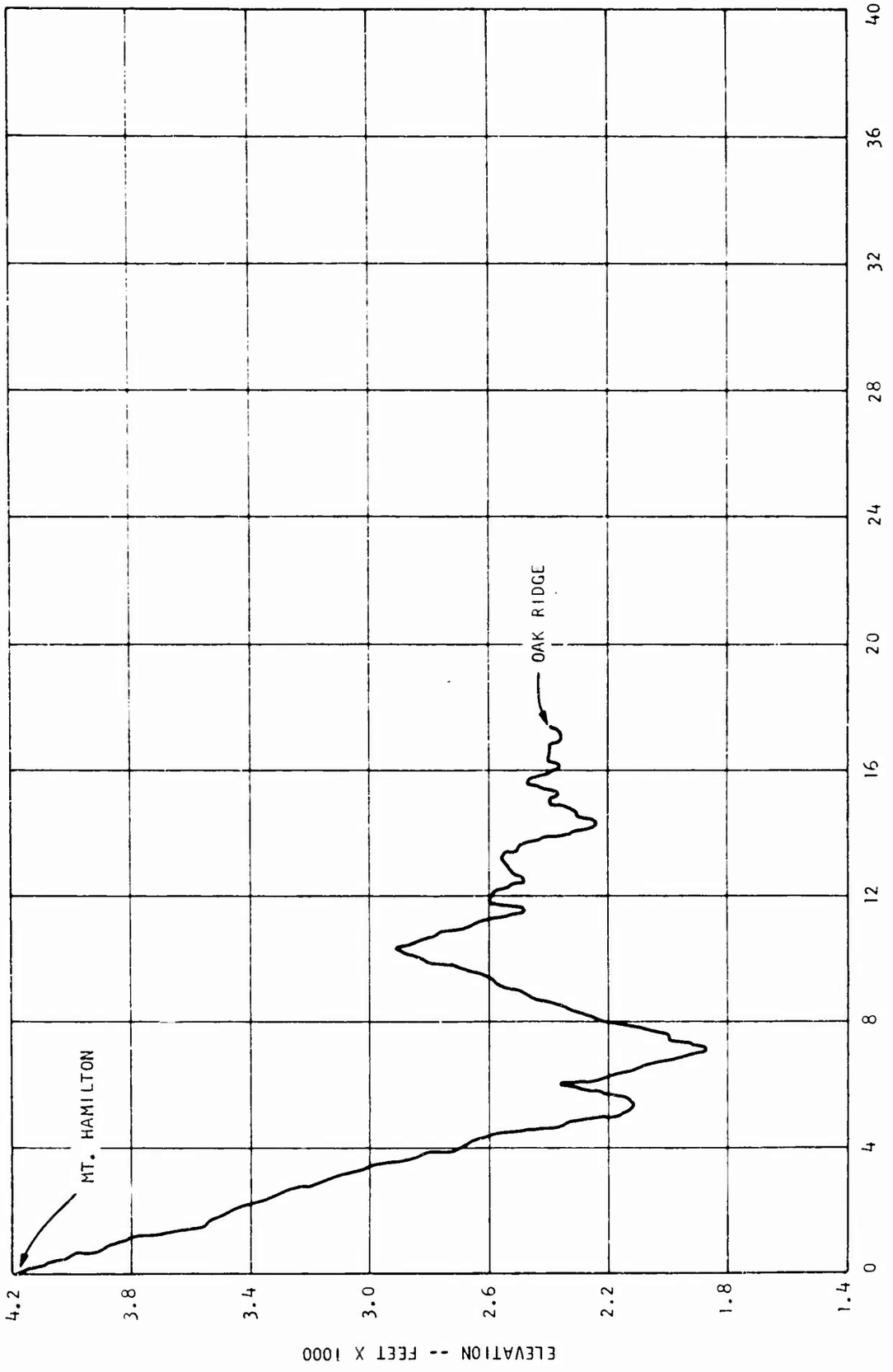

Figure 1h. Elevation Profile, Path 8.

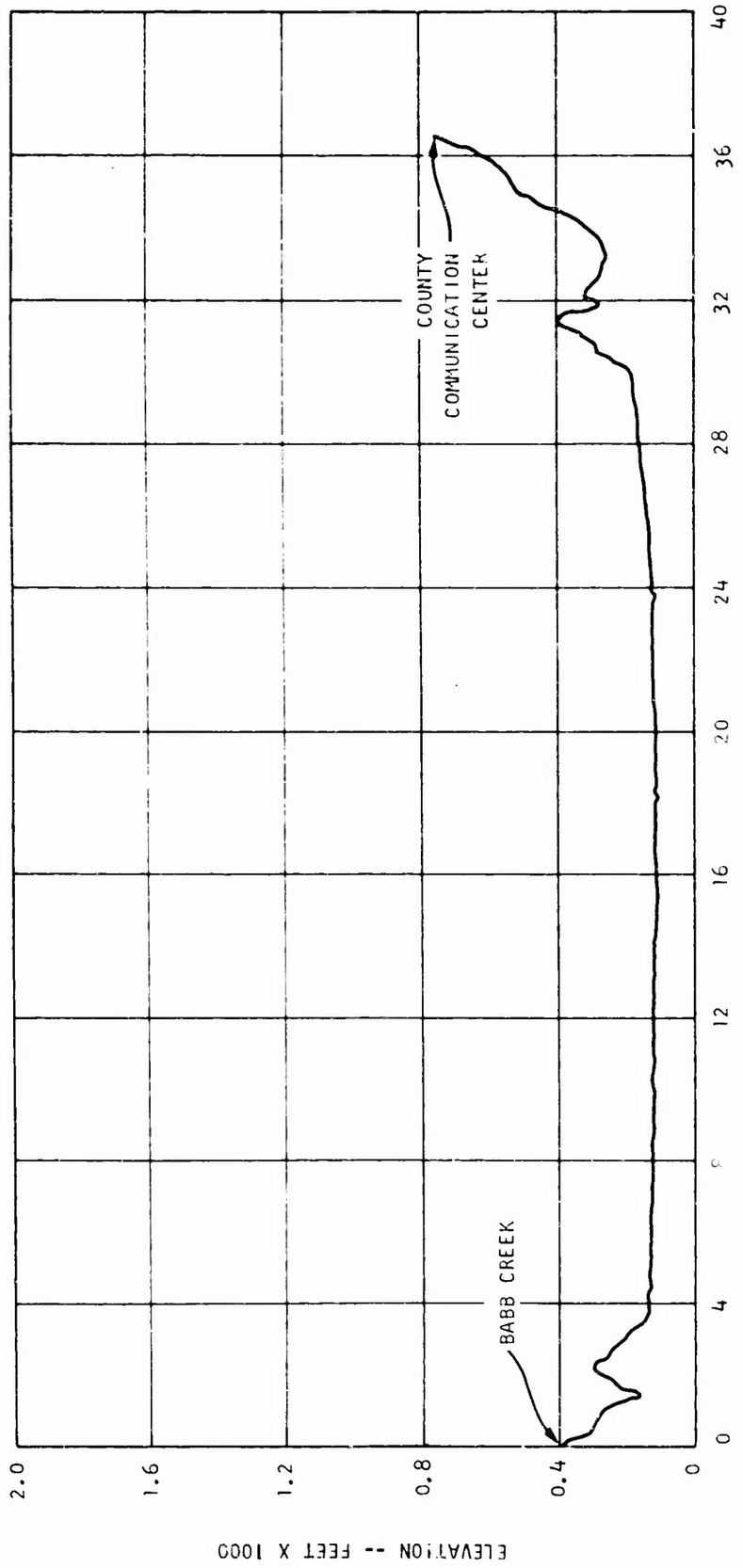

Figure 11. Elevation Profile, Path 9.

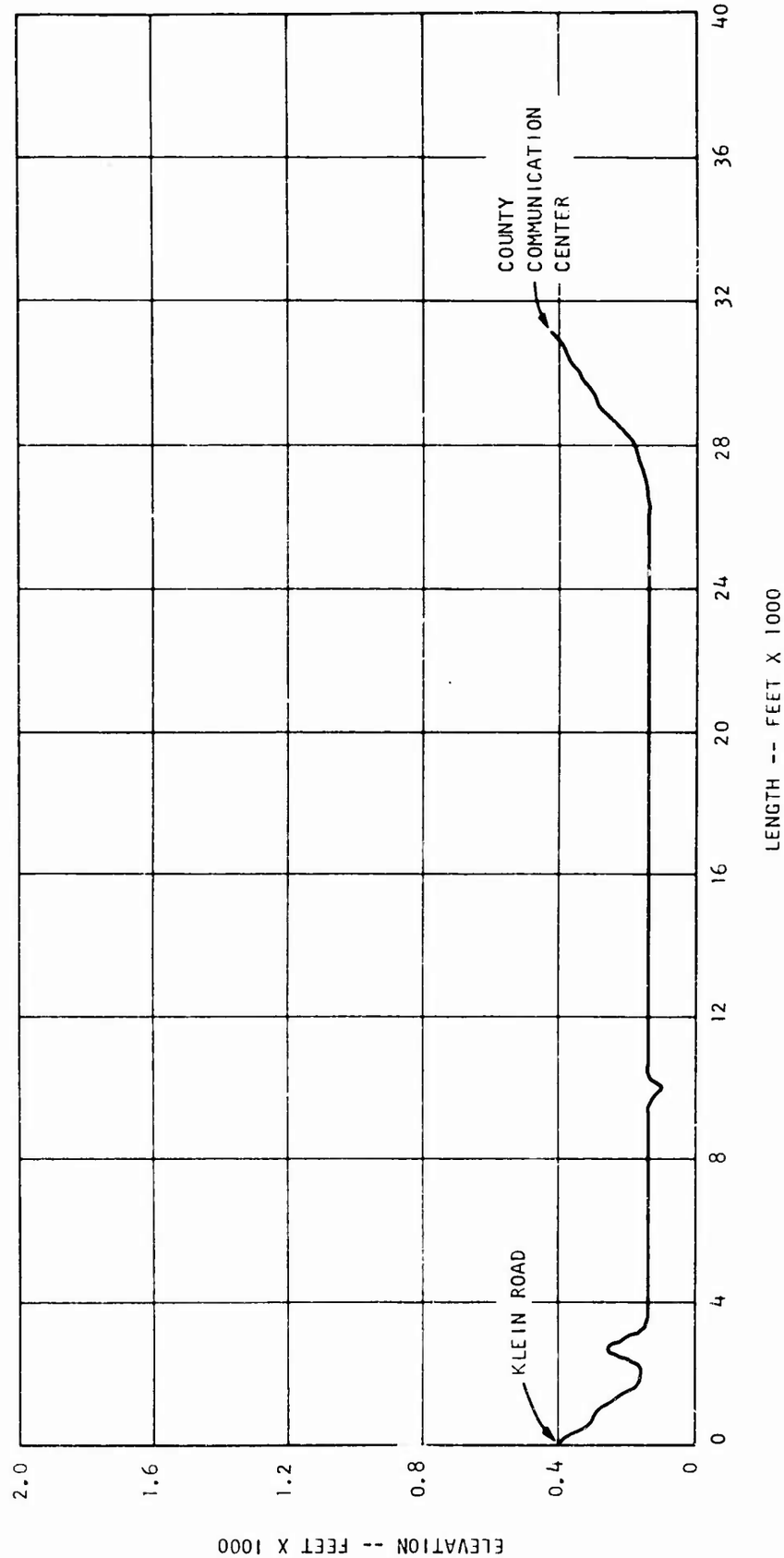

Figure 1j. Elevation Profile, Path 10.

Figure 2. Transmitting Site.

Figure 3. Receiving Site, Antenna Configuration.

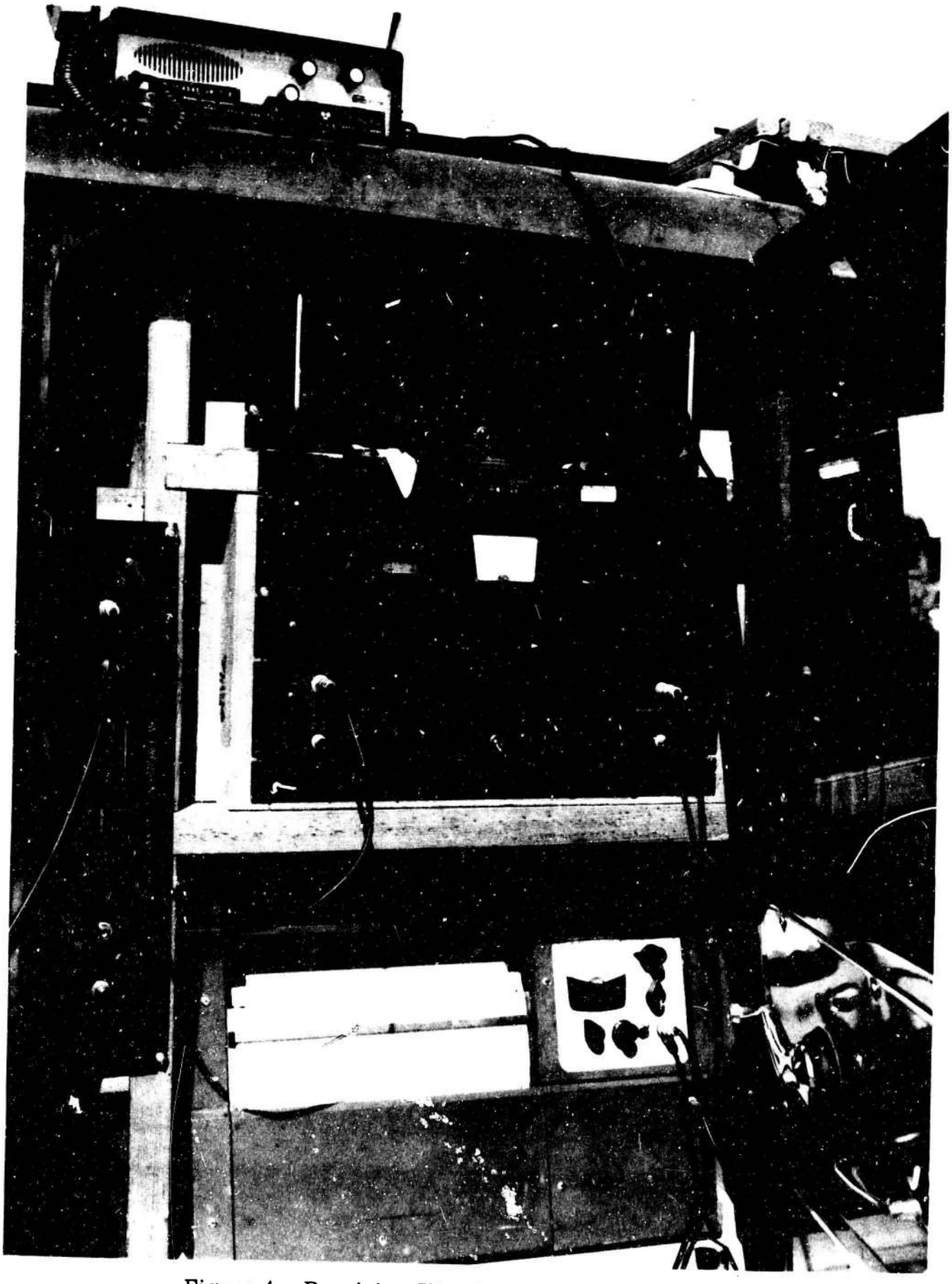

Figure 4. Receiving Site, Receiver and Recorder.

PATH 1A RUN 20 XMTR LOCATION 1A

DATE 5/17/65 TIME 1630 RCVR LOCATION Bielowski

XMTR HEIGHT _____ WEATHER Fair WIND Calm

GROUND Dry FOG -

Freq. (Mc)	Basic Loss (db)	Pwr. Ou (dbm)		Signal Level (dbm)	Measured Power (dbm)		Total Loss (db)		Δ Loss		Total Antenna Gain
					E	H	E	H	E	H	
120	88.67	38.0	E	max.	58.7	59.9	101.1	102.3	12.4	13.6	4.4
				min.	63.3	72.4	105.7	114.8	17.0	26.1	
		38.0	H	av.	59.9	64.7	102.3	107.1	13.6	18.4	
350	97.97	43.0	E	max.	63.4	65.3	117.6	119.5	19.6	21.5	11.2
				min.	69.5	88.3	123.7	142.5	25.7	44.5	
		43.0	H	av.	66.2	28.9	120.4	123.1	22.4	25.1	
750	104.61	38.0	E	max.	52.7	52.0	111.1	110.4	6.5	5.8	20.4
				min.	59.0	61.2	117.4	119.6	12.8	15.0	
		38.0	H	av.	55.2	55.2	113.6	113.6	9.0	9.0	
1000	107.09	37.0	E	max.	55.6	53.6	114.6	112.6	7.6	5.6	22.0
				min.	61.2	59.9	120.2	118.9	13.2	11.9	
		37.0	H	av.	57.8	56.8	116.8	115.8	9.8	8.8	
3000	116.67	26.6	E	max.	64.2	64.4	123.8	124.0	7.1	7.3	33.0
				min.	68.4	70.0	128.0	129.6	11.3	12.9	
		26.6	H	av.	66.7	67.5	126.3	127.1	9.6	10.4	
7500	124.61	20.3	E	max.	55.8	54.2	120.6	119.0	-4.0	-5.6	44.5
				min.	63.2	64.0	128.0	128.8	3.4	4.2	
		20.3	H	av.	59.1	58.2	123.9	123.0	-0.7	-1.6	
10.000	127.71		E	max.							
				min.							45.4
			H	av.							

REMARKS:

E Vertical Polarization

H Horizontal Polarization

Figure 5. Sample Data Sheet

4. --Continued

At 100 Mc, half-wave dipoles (gain approximately 2 db) were used at transmitter and receiver; at 350 Mc, a half-wave dipole was used at the receiver, while a log-periodic antenna (gain approximately 8 db) was used at the transmitter; for the 750-3000 Mc range, ridged horns were used at transmitter and receiver (gain ranging from 10 to 16 db); and for 7500 and 10,000 Mc, X-band horns were used (gain of 22 and 25 db). These antenna gains were checked both before and after the field tests to ensure ±1 db overall accuracy.

Section 5

DATA INTERPRETATION, REFLECTION COEFFICIENT

5.1 Specular and Diffuse Reflection Coefficients.

In the general case, the field measured while the receiving antenna is raised will contain two components: 1) a slowly varying sinusoid (i.e., large period) resulting from the interference of the direct wave, E_o, with the specularly reflected wave E_s, and 2) a rapidly varying sinusoid (small period) resulting from the interference of the diffuse component E_d with the resultant $E_o + E_s$.

5.1.1 Specular Component.

To determine the magnitude of the specular reflection coefficient, it was necessary to raise the receiver through at least one full period of field variation in the vertical plane. [If E_M and E_m are the maximum and minimum field values, respectively, over the period, the magnitude of the specular reflection coefficient, ρ_s, is expressed as

$$\left|\rho_s\right| = \frac{E_M/E_m - 1}{E_M/E_m + 1} \; .]$$

The period, P, for a transmitting antenna at height h_T located at some distance, d, from the receiving antenna, is

$$P = \frac{\lambda d}{2h_T} \; . \qquad (17)$$

The 24-foot height variation at the receiver allowed measurement of full periods or appreciable parts of periods for frequencies of 750 Mc and above. Accordingly, accurate measurements of ρ_s could be made over the interval

5.1.1 --Continued

750 to 10,000 Mc. At the two lower frequencies, only small portions of periods could be observed and, therefore, only estimates could be made as to the range of values for ρ_s.

5.1.1.1 750-10,000 Mc.

For the rough surfaces (paths 1 through 8), a specular component could be observed for essentially all paths. The surfaces with heavy vegetation (paths 1 through 5) appeared to have specular reflection coefficients of the same magnitude as, or even larger than, the less dense paths (6 through 8), although the magnitude of ρ_s was always small. Figure 6 shows the specular component for a variety of paths. It can be seen that, for the cases illustrated, the specular reflection coefficient, ρ_s, is never greater than 0.3 (maximum to minimum variation of 5 db), except for path 2 where ρ_s approaches 0.5. Table 2 presents the results in a slightly different form. Here path difference between direct and reflected wave (from the highest point of the surface near the center of the first Fresnel zone) is compared with the magnitude of the specular reflection coefficient.

Table 2. Path Difference Versus Specular Reflection Coefficient

Path	Path Difference	Frequency (Mc)	Specular Reflection Coefficient, ρ_s
1A	2.95	3000	0.23
2	8.90	7500	0.50
4	40.00	3000	0.30
8	3.90	3000	0.15

One would expect that increasing the path difference would result in the surface appearing rougher and in a drop in the value of ρ_s; however, this effect does not appear in the table. No apparent trend, relating ρ_s to either density of vegetation or path difference between direct and reflected wave, is evident.

At these higher frequencies, little difference between the values of the specular reflection coefficient was noted for the smooth, vegetation-free paths (9 and 10). Figure 7 shows typical results for these two paths. For path 9,

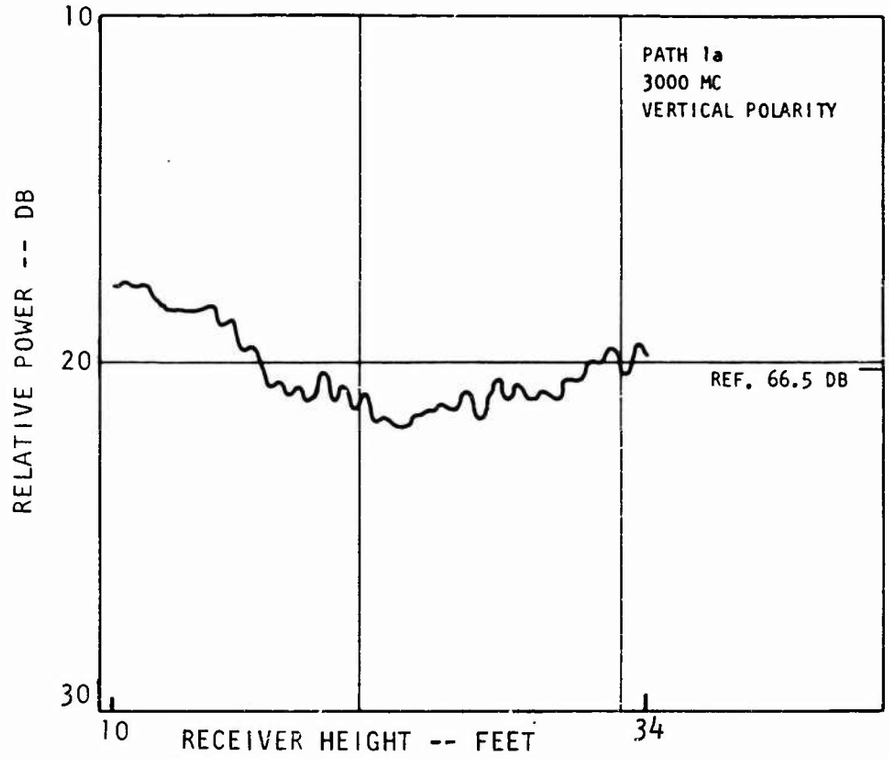

Figure 6a. Specular Component for Path 1A.

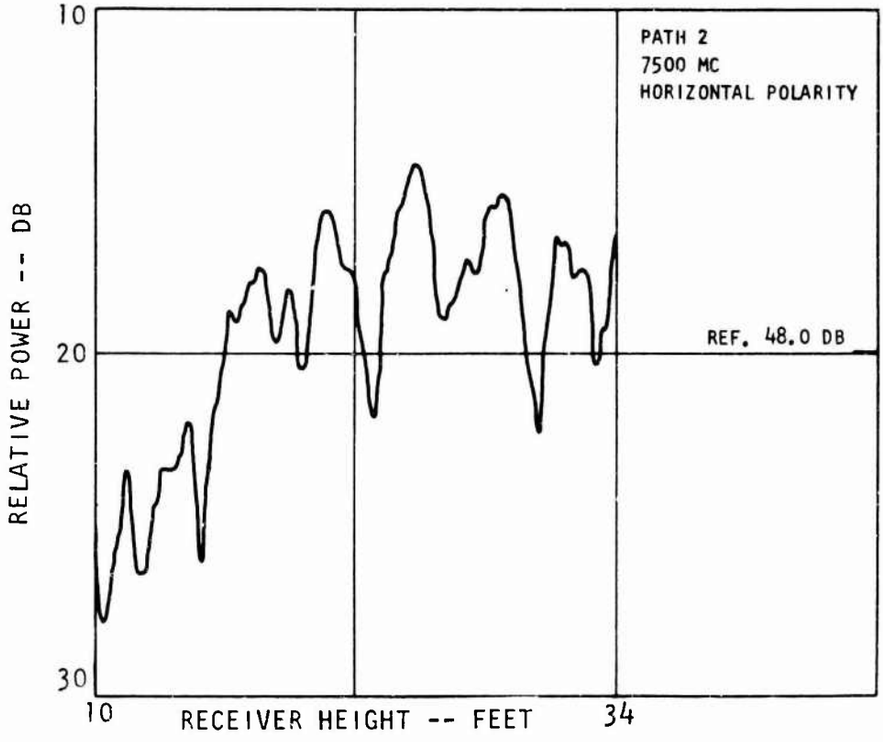

Figure 6b. Specular Component for Path 2.

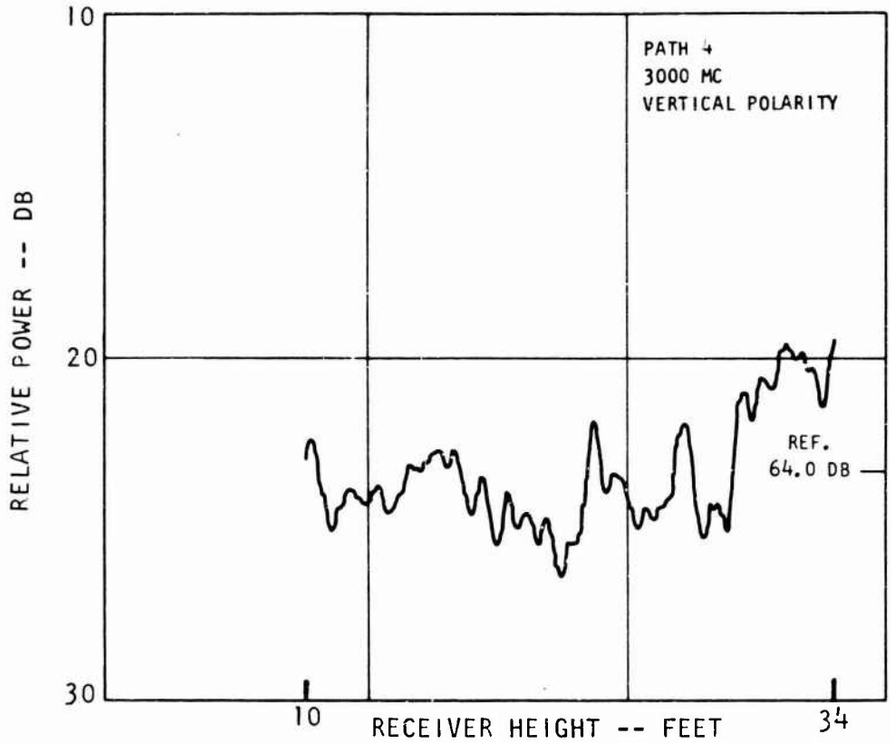

Figure 6c. Specular Component for Path 4.

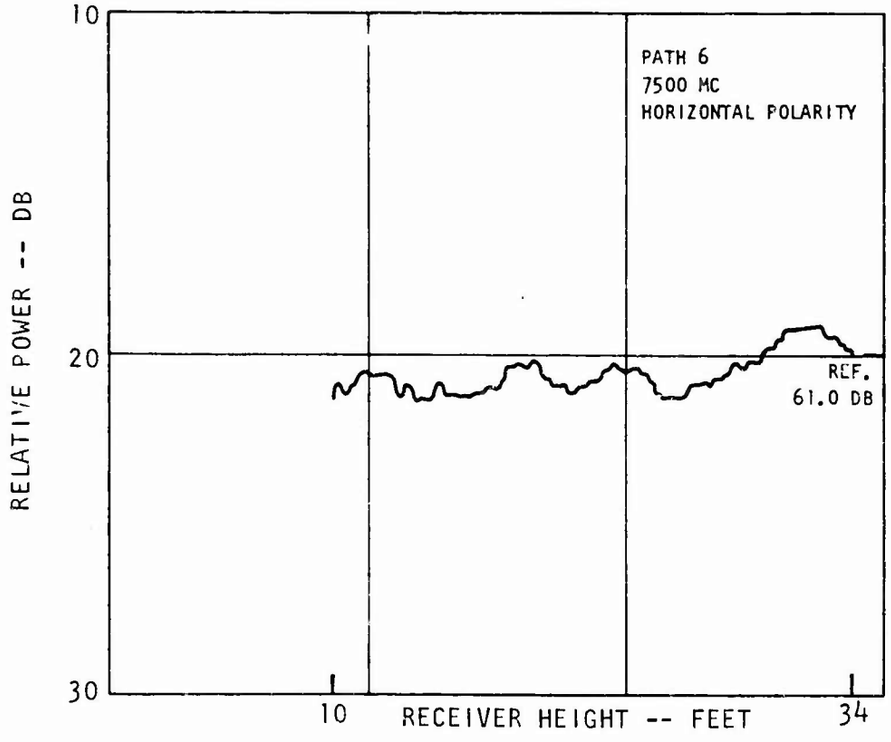

Figure 6d. Specular Component for Path 6.

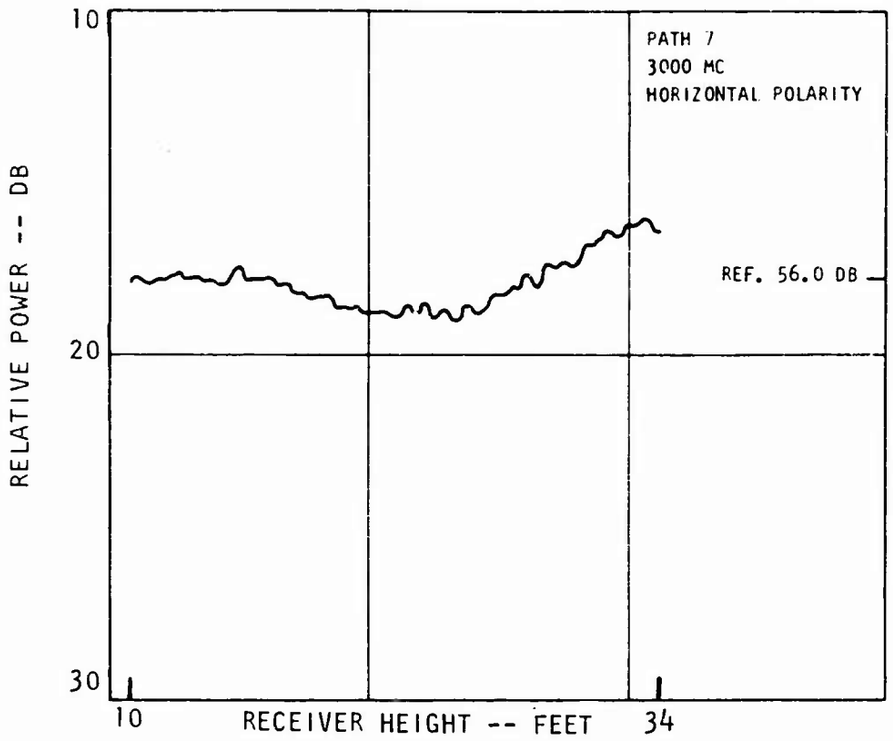

Figure 6e. Specular Component for Path 7.

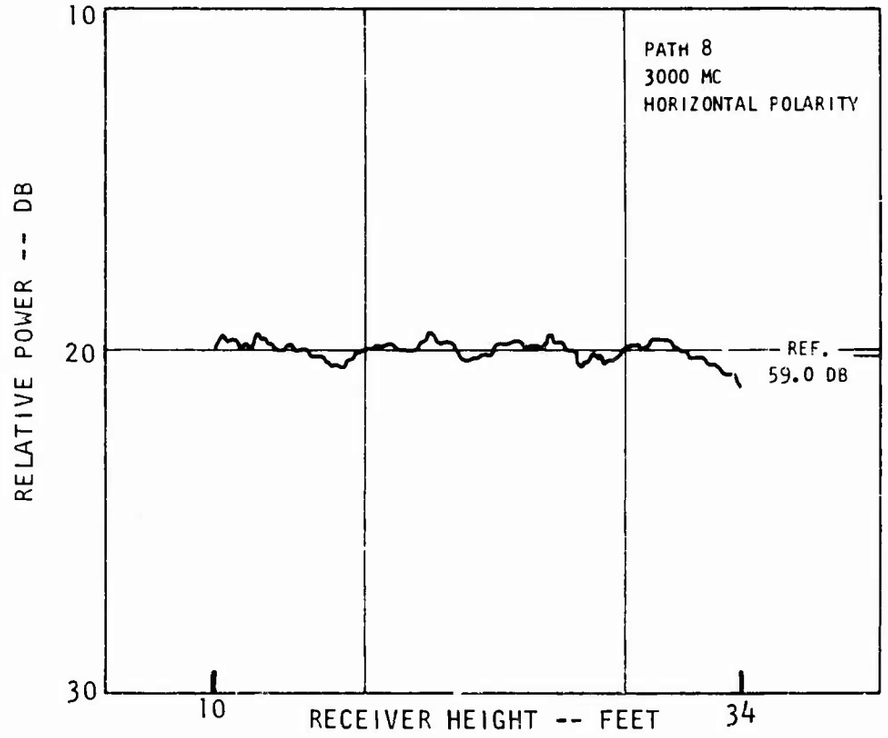

Figure 6f. Specular Component for Path 8.

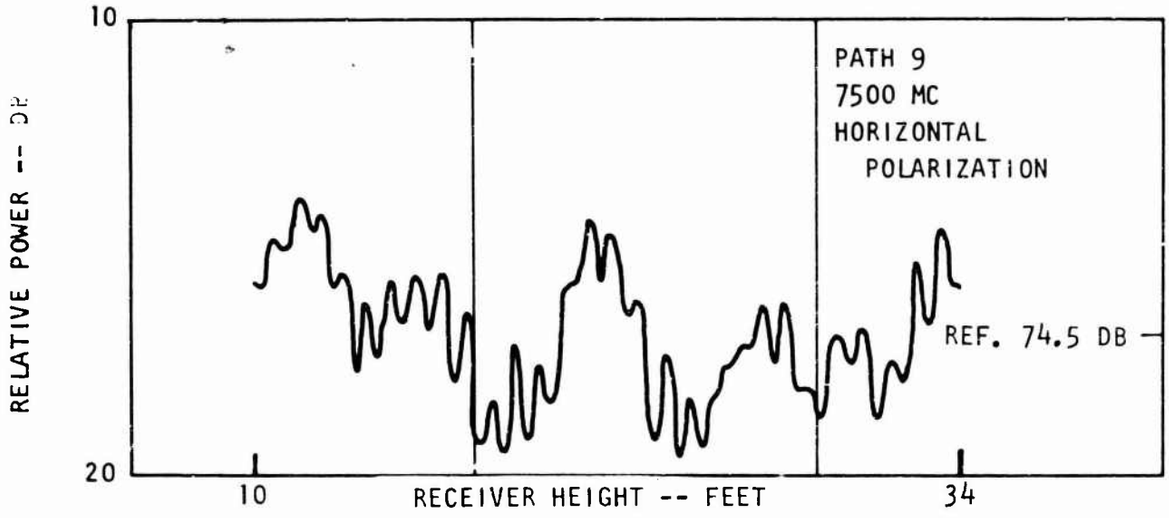

Figure 7a. Specular Component for Smooth Path 9.

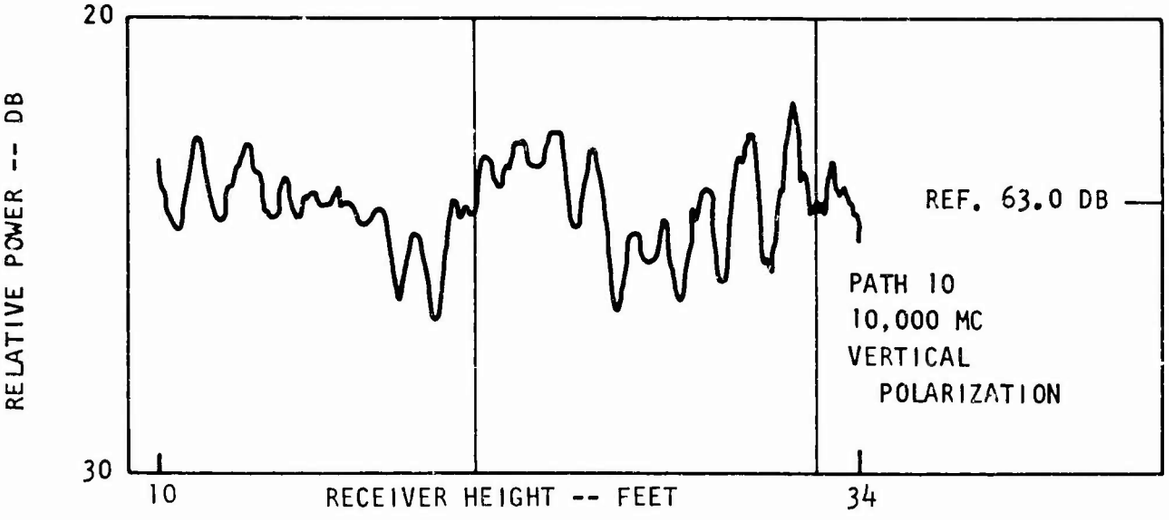

Figure 7b. Specular Component for Smooth Path 10.

5.1.1.1 --Continued

ρ_s equals 0.30, while for path 10, ρ_s is about 0.23. These values are approximately equal to those observed on paths 1A and 4, paths which are very rough. Thus at the higher frequencies, all paths regardless of roughness or irregularity appear "rough," with values of ρ_s tending to cluster between 0.20 and 0.30, and almost always less than 0.5.

5.1.1.2 100-350 Mc.

At these frequencies, the magnitude of the specular reflection coefficient is large. The fluctuations in the specular field result in nulls in the gain-height curve whose depths regularly range from 10 to 20 db over most paths. These fluctuations may arise from variation of the vertical gradient of the atmospheric index of refraction or multipath effects in the atmosphere. Examples of the types of nulls encountered are shown in Figure 8 for a path with dense vegetation (path 1A) and one with sparse vegetation (path 6). Table 3 gives the null depth for vertical and horizontal polarization for 100 and 350 Mc for the rough paths.

Table 3. Null Depth Versus Frequency for the Rough Paths.

Path	100 Mc		350 Mc	
	Vertical (db)	Horizontal (db)	Vertical (db)	Horizontal (db)
1	7	12	11	9
1A	6	13	6	23
2	7	6	3	7
3	11	16	12	9
4	2	18	13	11
5	11	5	10	10
6	*	*	3.5	22
7	*	*	10	7
8	*	*	22	20

* Measurements at 100 Mc are not possible over these paths due to heavy interferenee.

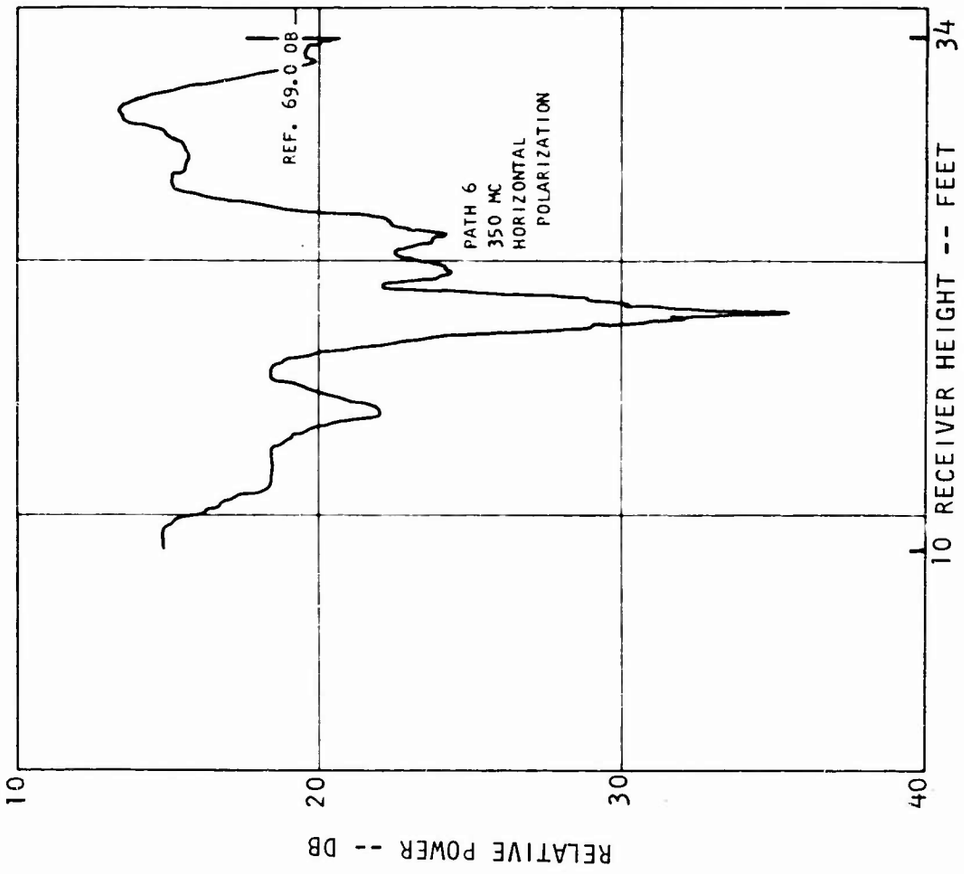

Figure 8b. Path 6, Sparse Vegetation in Comparison of Specular Components for Paths with Dense Versus Sparse Vegetation

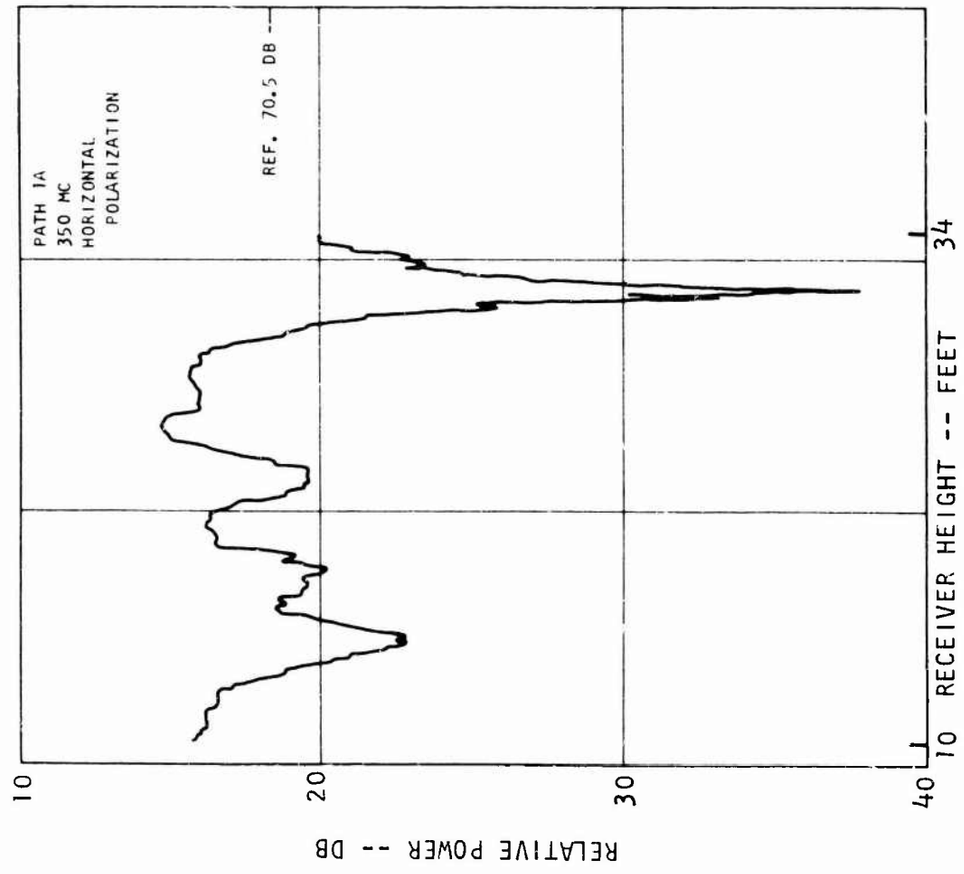

Figure 8a. Path 1A, Dense Vegetation in Comparison of Specular Components for Paths with Dense Versus Sparse Vegetation

5.1.1.2 --Continued

Of interest is the fact that the magnitude of the nulls does not always correlate with the magnitude of the specular reflection coefficient measured at the higher frequencies. Path 8, which showed a ρ_s of 0.15 at 3.0 Gc, exhibited nulls of over 20 db at 350 Mc (Figure 9), while path 2, which indicated a specular reflection coefficient of about 0.50 at 7.5 Gc, showed variation of only 7 db at 350 Mc (Figure 10).

The null depths observed for horizontal polarization are, in general, more severe than for vertical, as is to be expected with the reflection coefficient being somewhat greater for horizontal polarization than for vertical polarization. The actual value of the reflection coefficient for the two polarizations could not be determined because of limitations on receiver height variation, but the deep nulls indicate values well in excess of 0.50.

5.1.2 Diffuse Component, 750 - 10,000 Mc.

The variations of the rapidly oscillating component could be readily observed over this entire frequency interval. The magnitude of these oscillations in general decreases as the frequency increases. A typical example is shown in Figure 11 for path 1A where height-gain curves are shown for frequencies from 750 to 7500 Mc. The magnitude of the reflection coefficient for the rapidly oscillating component, hereafter called diffuse, varies from a maximum of 0.30 at 750 Mc to 0.13 at 7500 Mc. For the other rough paths, the diffuse reflection coefficient, ρ_d, rarely exceeds 0.50. Table 4 indicates how ρ_d varies with path and frequency. An exception to the general case occurs for path 3 when the reflection coefficient increases with increasing frequency; this is shown in Figure 12.

One may consider the fluctuations of the specular field to tend to become Rayleigh-distributed as the magnitude of the reflection coefficient gets smaller, i.e., to fluctuate in the same manner as the diffuse component. Thus, what is referred to as the diffuse component also contains the variations of the specular component. The individual contributions of the specular and diffuse fluctuations to the rapidly oscillating component of the field is unknown.

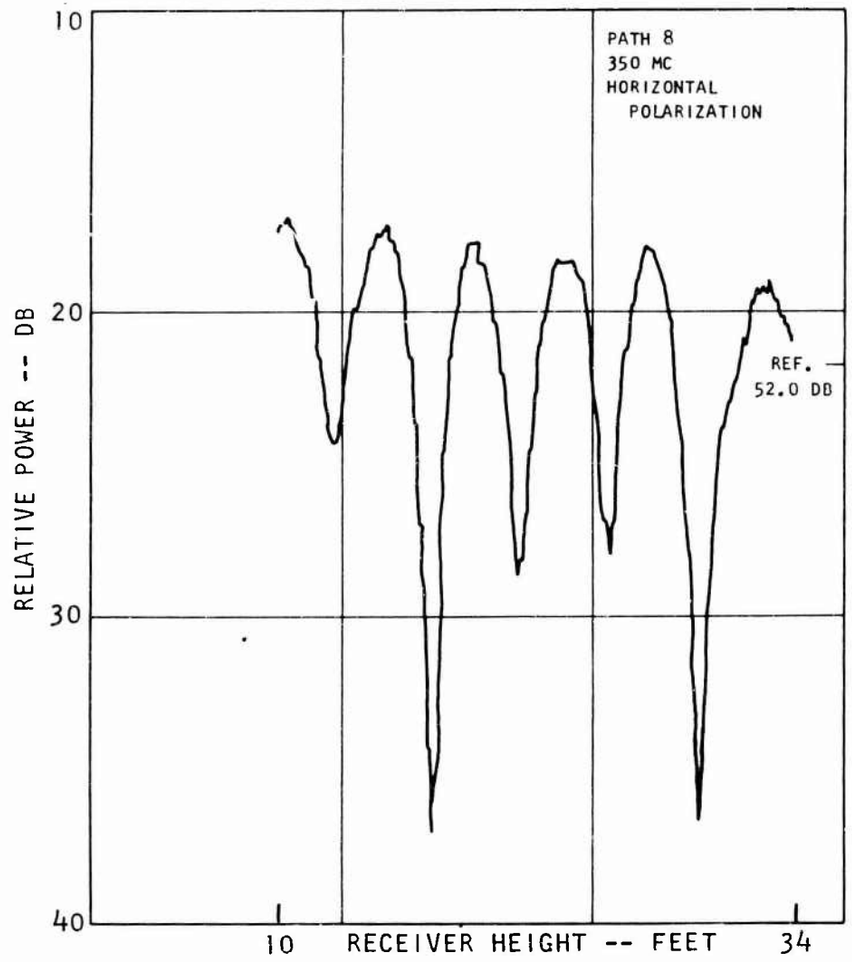

Figure 9a. Specular Component for Path 8 at 350 Mc, Vertical Polarization.

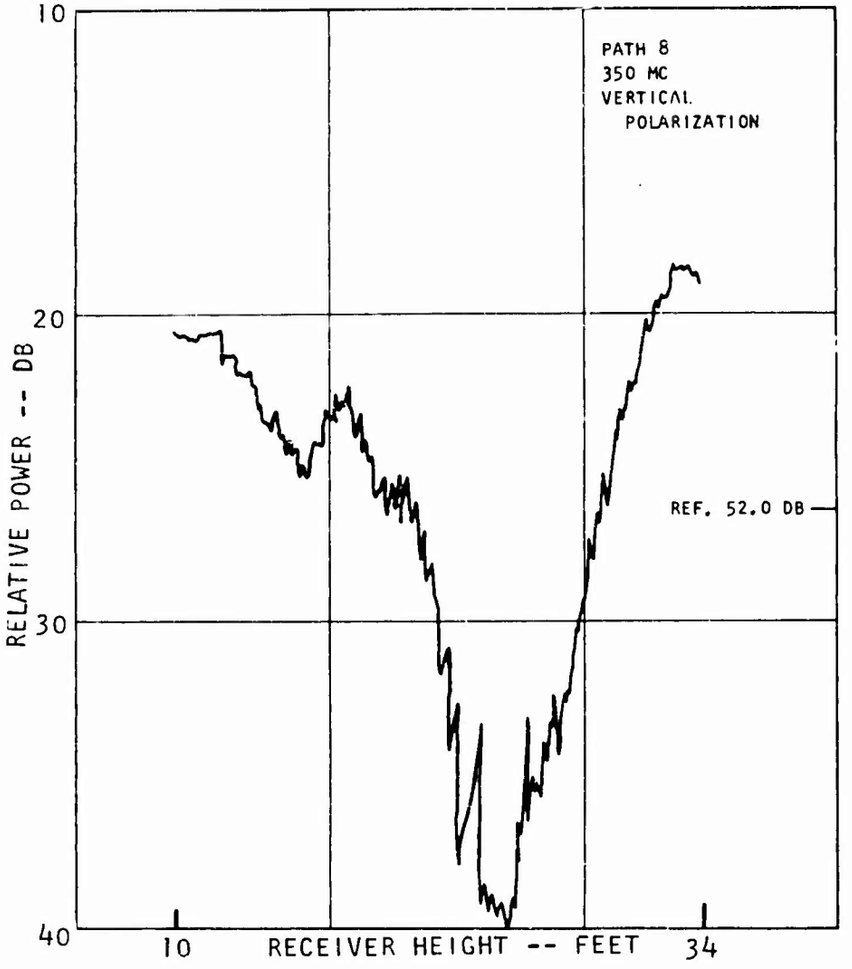

Figure 9b. Specular Component for Path 8 at 350 Mc, Horizontal Polarization.

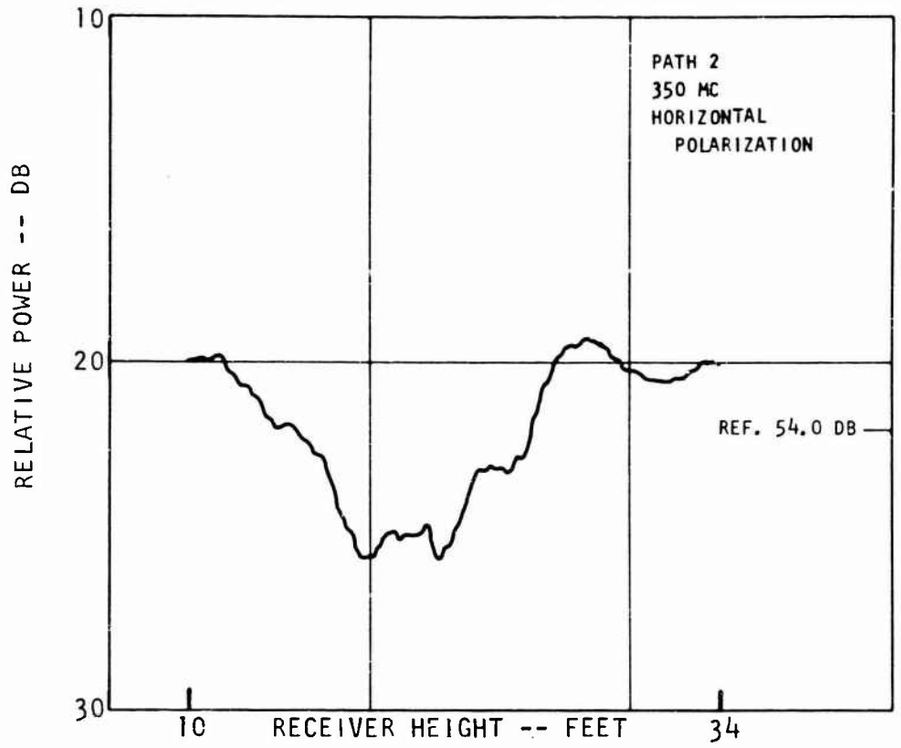

Figure 10. Specular Component for Path 2 at 350 Mc, Horizontal Polarization.

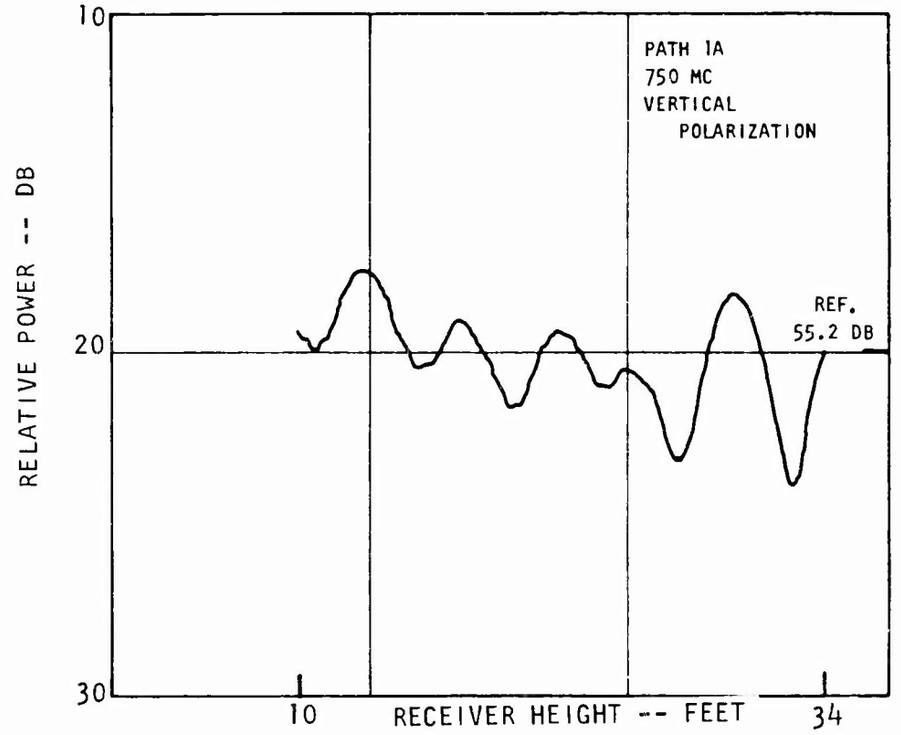

Figure 11a. Diffuse Component for Path 1A, 750 Mc Vertical.

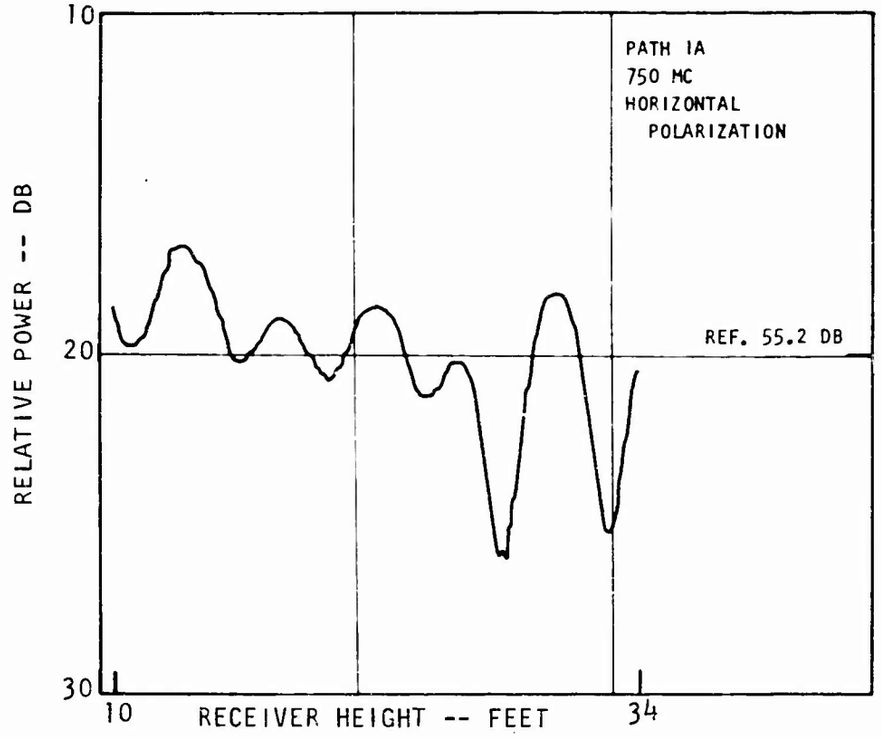

Figure 11b. Diffuse Component for Path 1A, 750 Mc Horizontal.

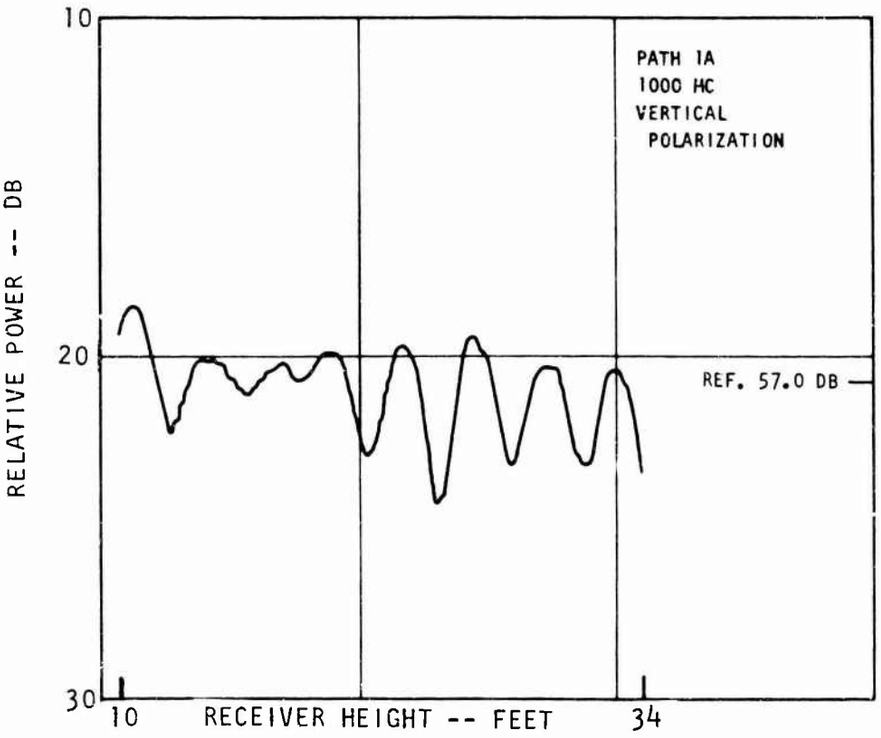

Figure 11c. Diffuse Component for Path 1A, 1000 Mc Vertical.

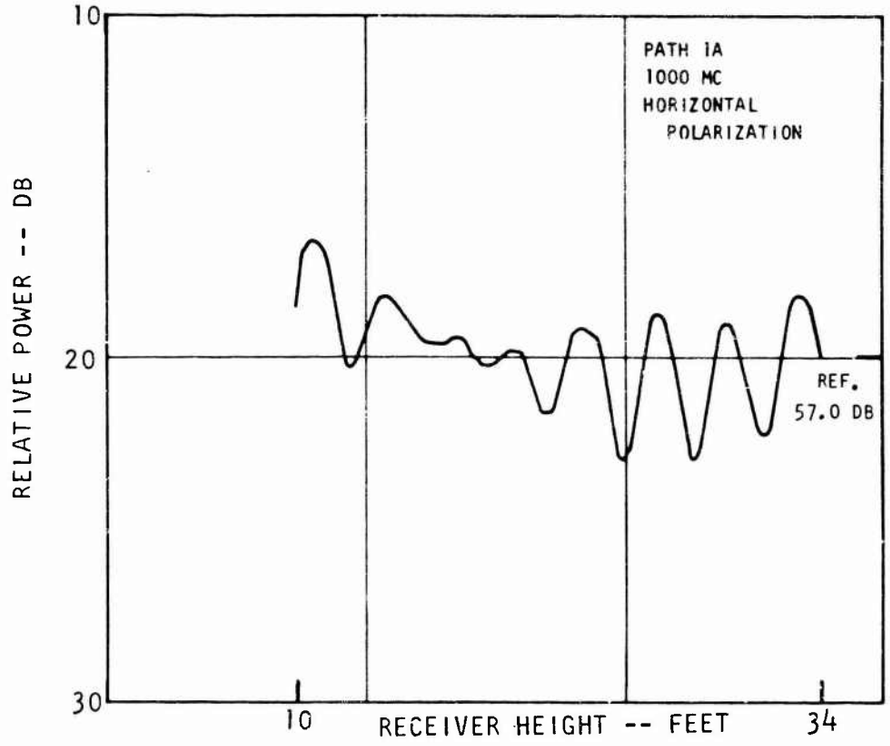

Figure 11d. Diffuse Component for Path 1A, 1000 Mc Horizontal.

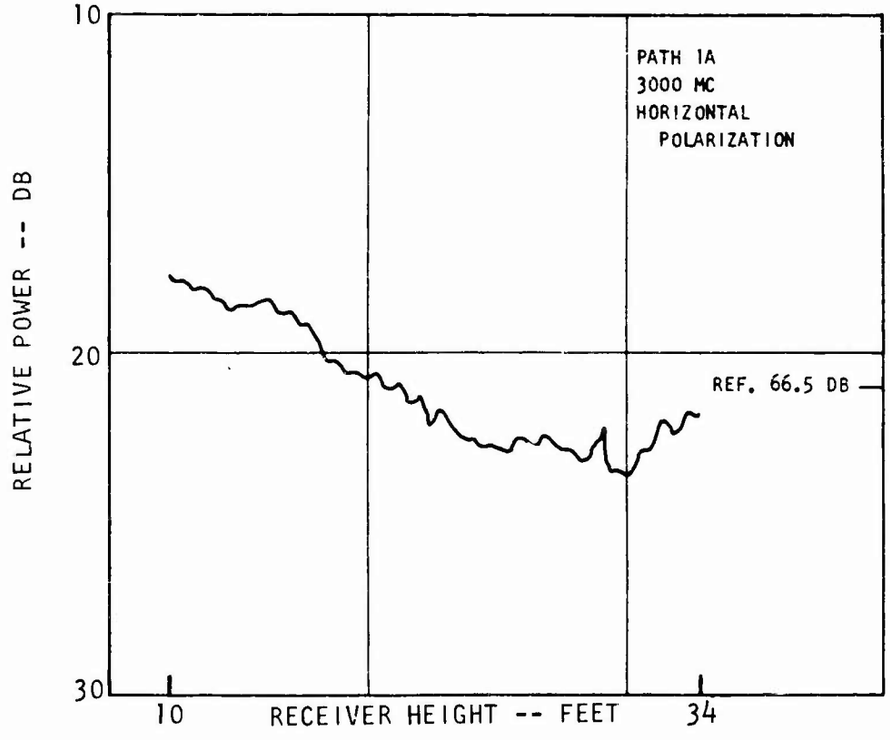

Figure 11c. Diffuse Component for Path 1A, 3000 Mc Horizontal.

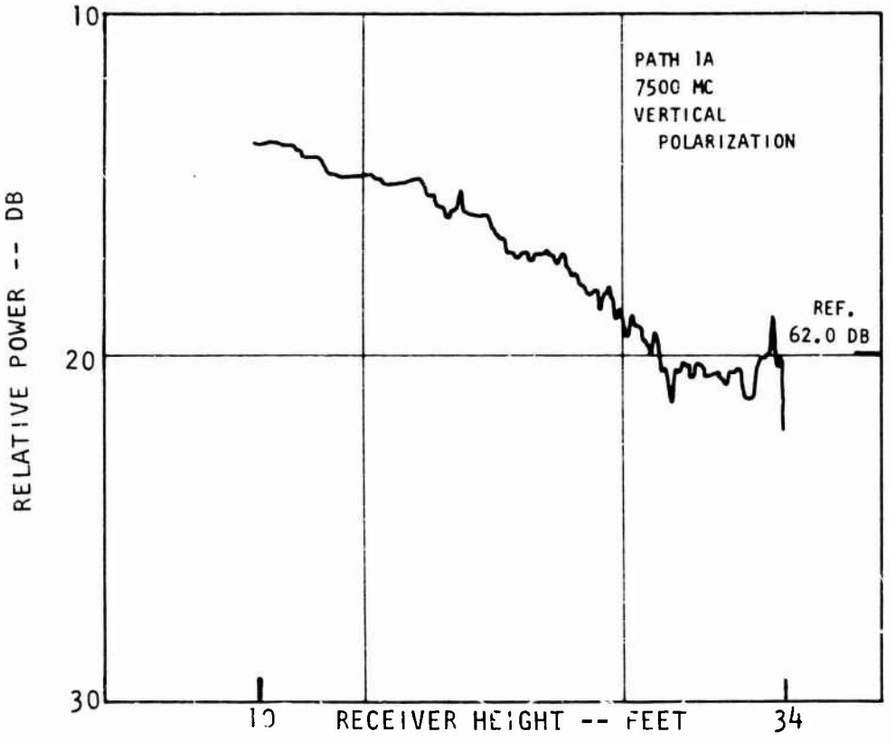

Figure 11f. Diffuse Component for Path 1A, 7500 Mc Vertical.

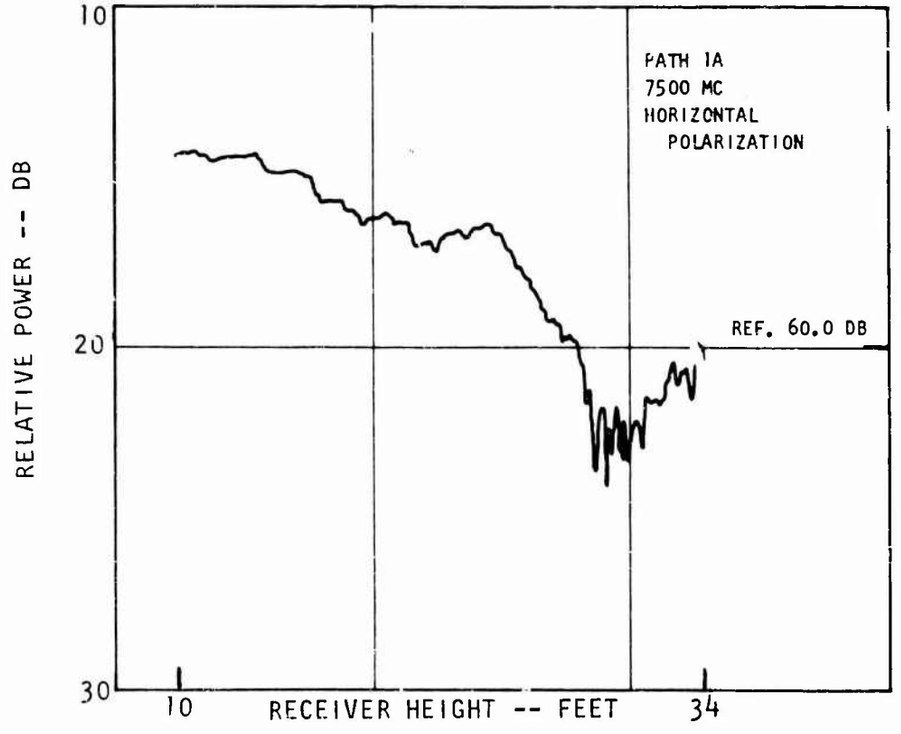

Figure 11g. Diffuse Component for Path 1A, 7500 Mc Horizontal.

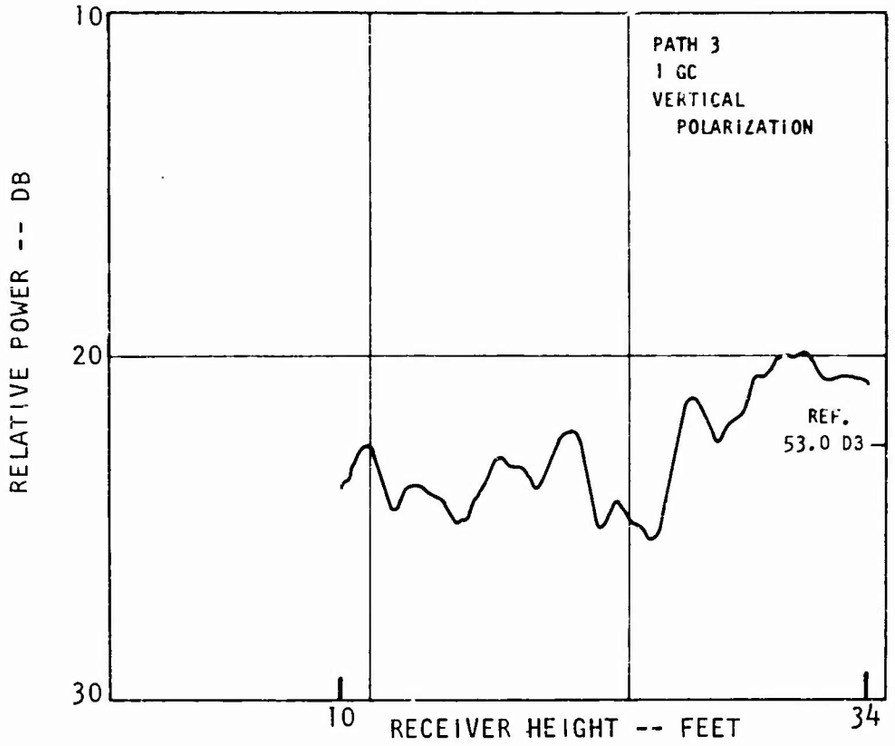

Figure 12a. Diffuse Component Path 3, Reflection Coefficient Variation as a Function of Frequency, 1 Gc Vertical

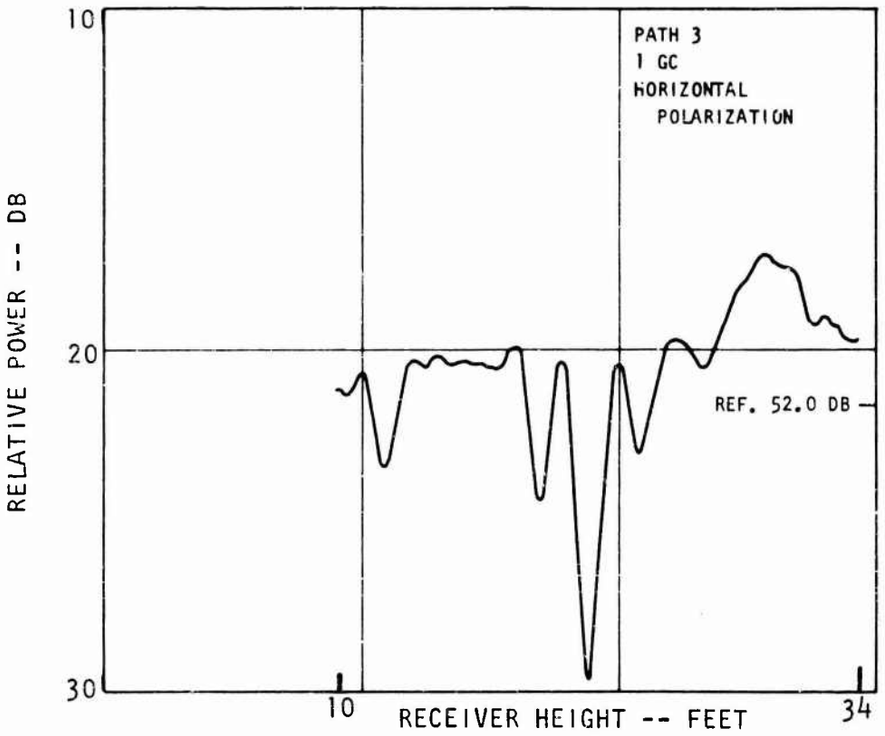

Figure 12b. Diffuse Component Path 3, Reflection Coefficient Variation as a Function of Frequency, 1 Gc Horizontal

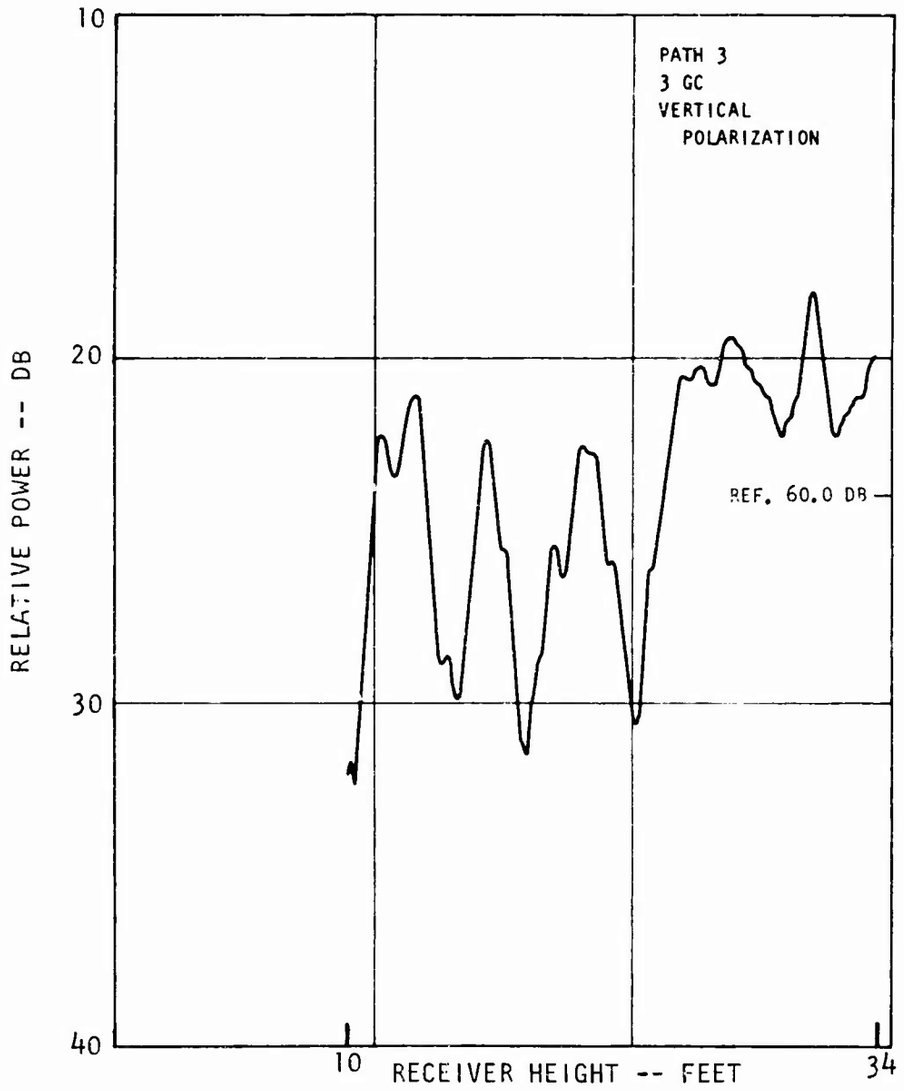

Figure 12c. Diffuse Component Path 3, Reflection Coefficient Variation as a Function of Frequency, 3 Gc Vertical

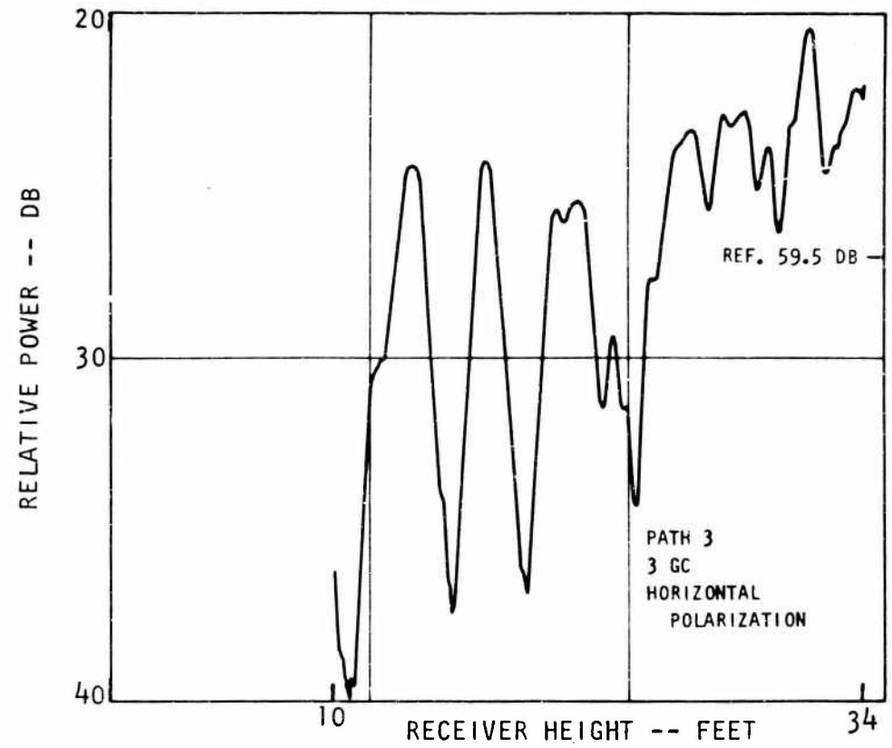

Figure 12d. Diffuse Component Path 3, Reflection Coefficient Variation as a Function of Frequency, 3 Gc Horizontal

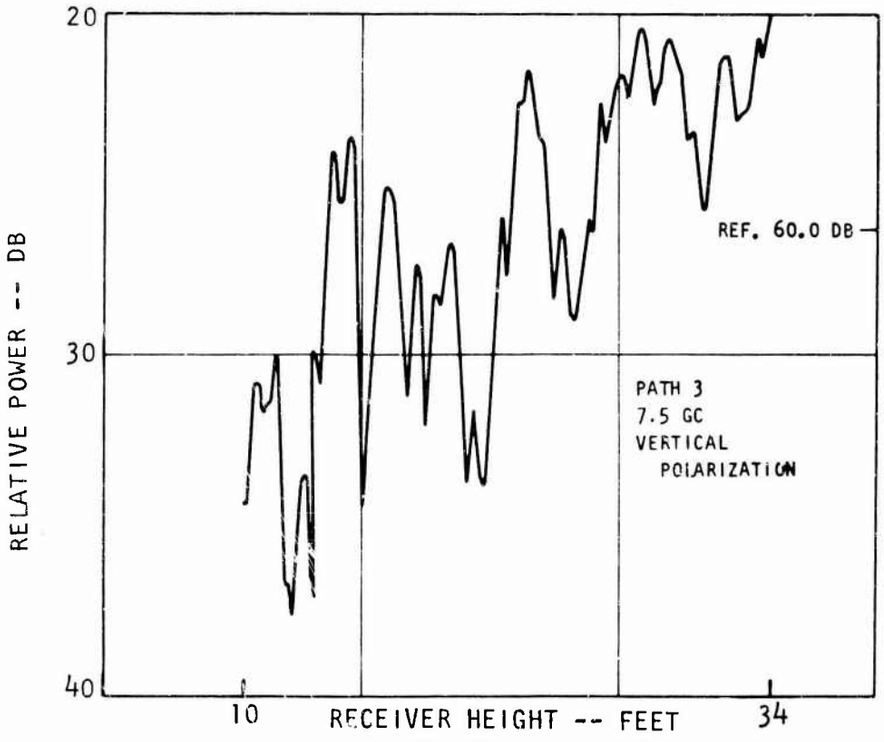

Figure 12e. Diffuse Component Path 3, Reflection Coefficient Variation as a Function of Frequency, 7.5 Gc Vertical

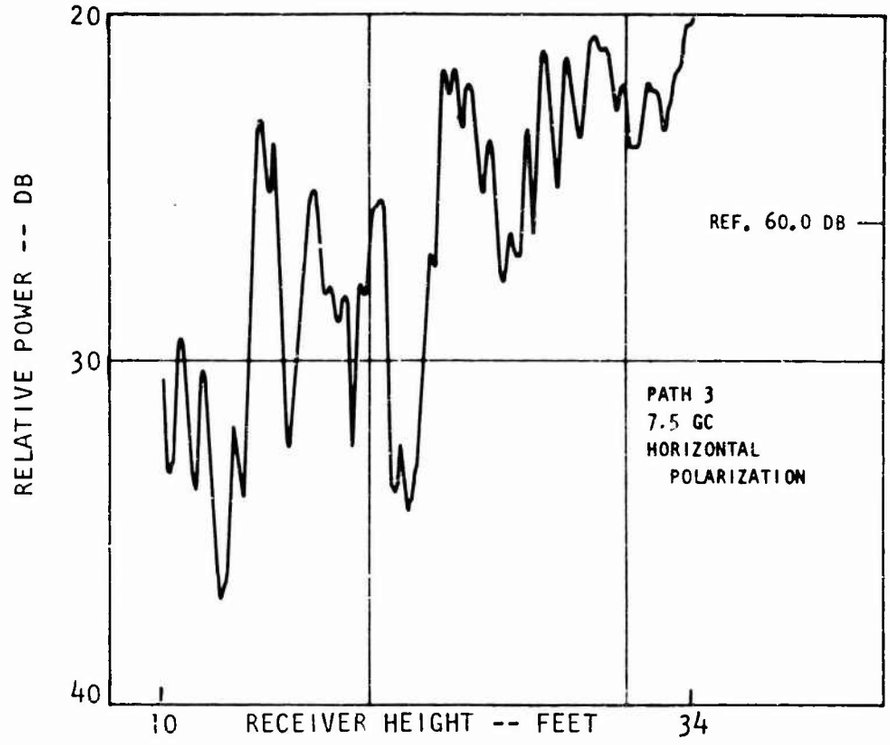

Figure 12f. Diffuse Component Path 3, Reflection Coefficient Variation as a Function of Frequency, 7.5 Gc Horizontal

Table 4. Path and Frequency Variation of ρ_d

Path	Frequency (Mc)	ρ_d	Variation of ρ_d
1	750 to 7500 3000	0.50 to 0.23 0.17	Gradual drop with increasing frequency Sharp drop at this point
1A	750-10,000	0.43 to 0.20	Continual decrease with increasing frequency
2	750-10,000	0.30 to 0.50	Large at all frequencies, no trend
3	3000 and 7500 750 and 1000	0.60 to 0.20	Larger at higher two frequencies
4	750-10,000	0.40 to 0.20	Gardual decrease with increasing frequency
5	750	0.17 to 0.11	Maximum at this frequency Small at all frequencies
6	750-10,000	0.20 to 0.10	Small at all frequencies Decreases with increasing frequency
7	750-10,000		Decreases with increasing frequency
8	750-10,000	0.20 to 0.10	Small at all frequencies

Section 6

DATA INTERPRETATION, PROPAGATION LOSS

The results of the measurements are presented in several forms. Figure 13 plots the average of the runs for each path, showing maximum, minimum, and mean loss (with respect to effective free-space loss) as a function of distance for each frequency. Vertical and horizontal polarization are plotted on the same curve for a given frequency. No difference in these results is apparent for the two transmitter heights. Path 1 (18,000 feet), path 1A (16,800 feet), and path 2 (15,500 feet), all with small grazing angle and dense vegetation, usually show loss greater than the mean, M, for the group as a whole. The range from maximum to minimum (i.e., the magnitude of the oscillations) is about the same for these paths as for the others. Paths 3 through 8 and 10 show little difference in mean loss above effective free-space loss, while path 9 generally has less loss than the group average. The average loss for a given frequency above effective free-space loss varies so little over the various distances that it may be considered independent of path length.

Figures 14 and 15 show path loss as a function of frequency for each of the paths: Figure 14 considers vertical polarization and Figure 15 horizontal polarization. For frequencies of 750 Mc and above for both polarizations, the average loss above effective free-space loss decreases with increasing frequency. At 750 Mc the average loss above effective free-space loss is about 8 db, while at 10,000 Mc there is a gain of about 5 db. At 100 Mc the average loss is greater than 10 db, while at 300 Mc the average loss approaches 20 db above effective free-space loss. The decrease in loss for the paths with little vegetation is more pronounced than for those with dense growth, although it is present for the latter paths also. The unusually large loss at 300 Mc is present for all paths, but its cause is not yet understood.

Figure 16 gives a plot of the mean and standard deviation for the average loss for all paths as a function of frequency. The trends indicated in Figures 14 and 15 are more readily seen. Little difference can be observed in Figure 16 between horizontal and vertical polarization as the frequency exceeds 750 Mc.

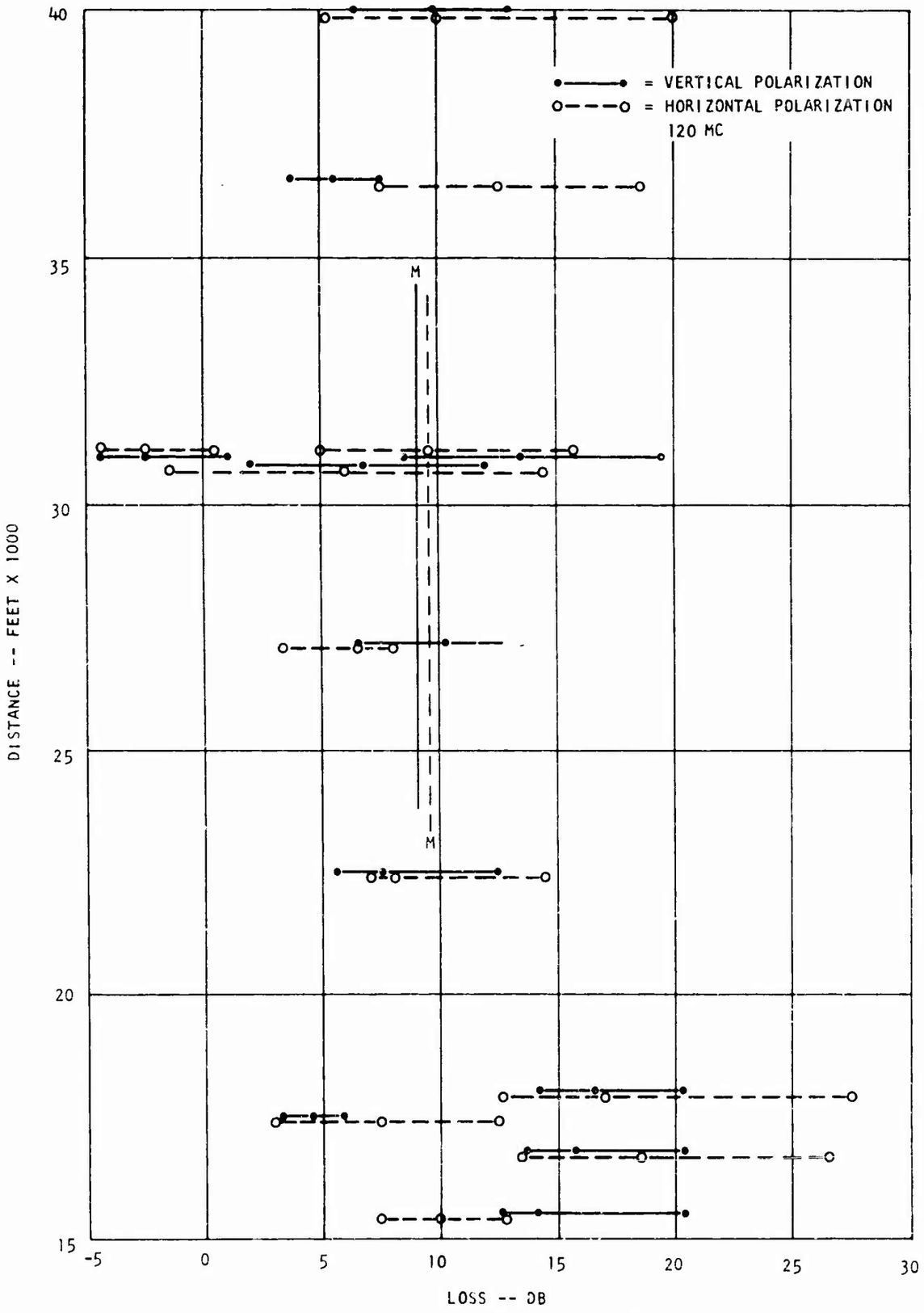

Figure 13a. Propagation Loss Plots: Maximum, Minimum, and Mean Loss as a Function of Distance for Each Frequency, Loss at 120 Mc.

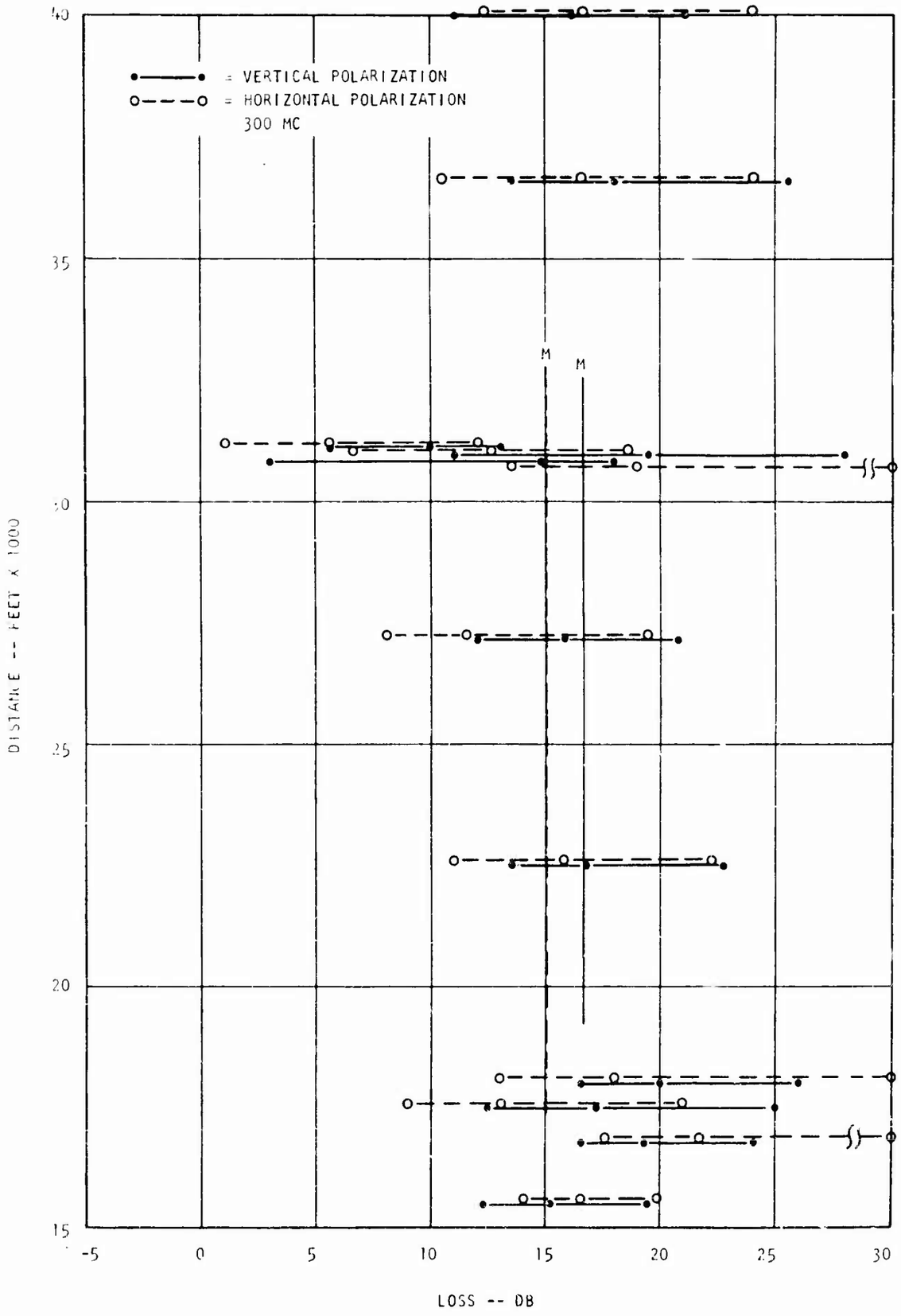

Figure 13b. Propagation Loss Plots, Loss at 300 Mc.

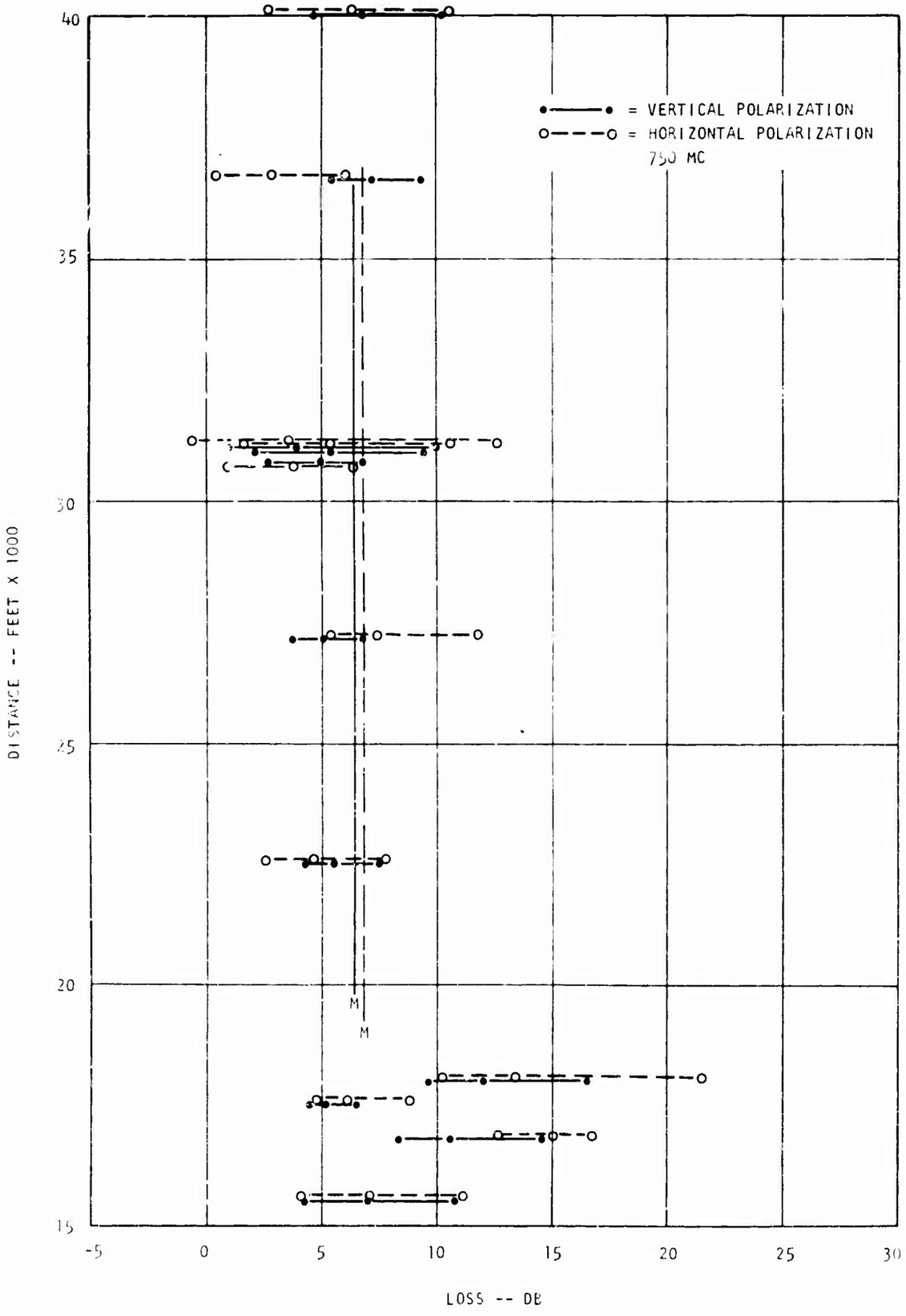

Figure 13c. Propagation Loss Plots, Loss at 750 Mc.

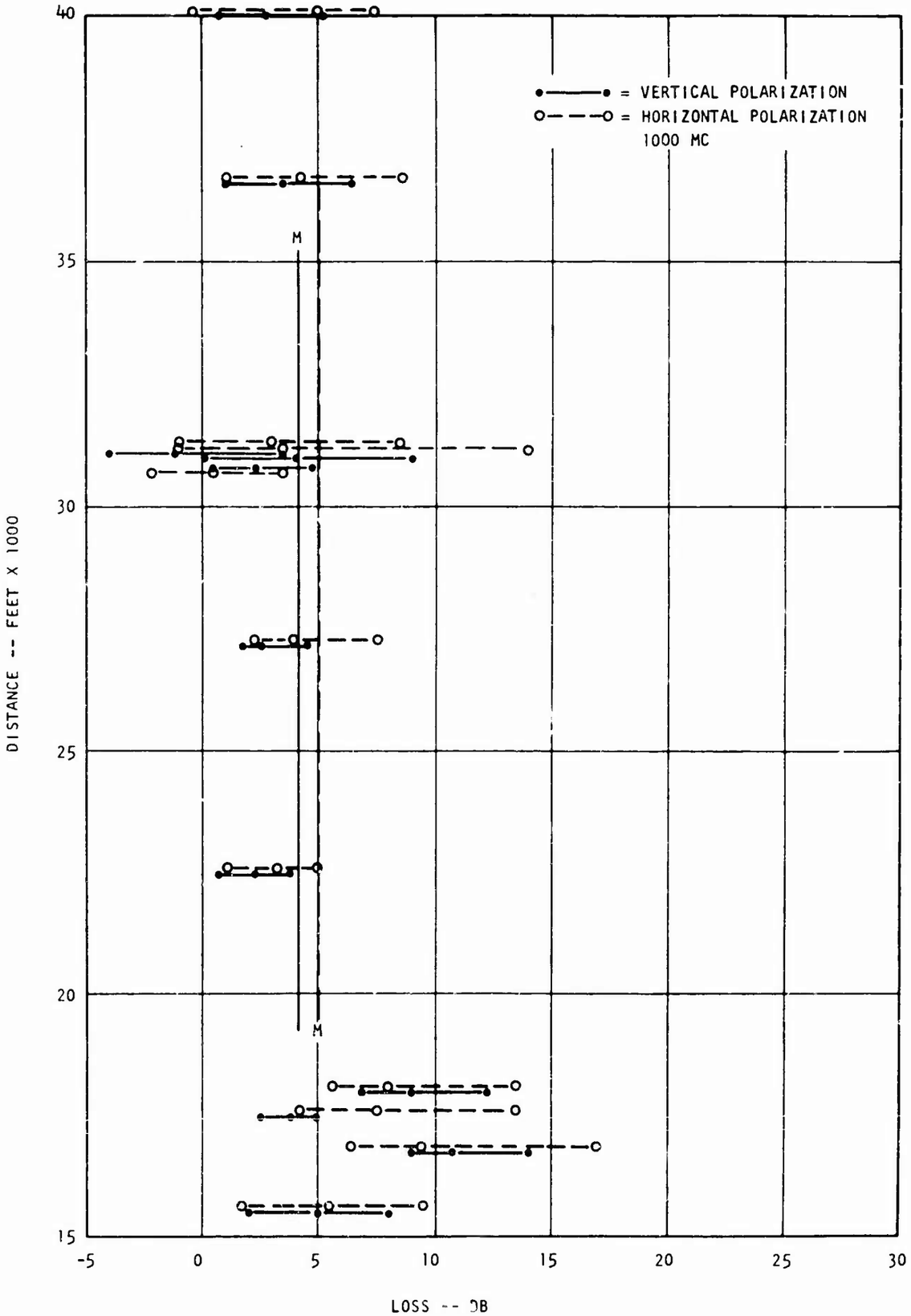

Figure 13d. Propagation Loss Plots, Loss at 1000 Mc.

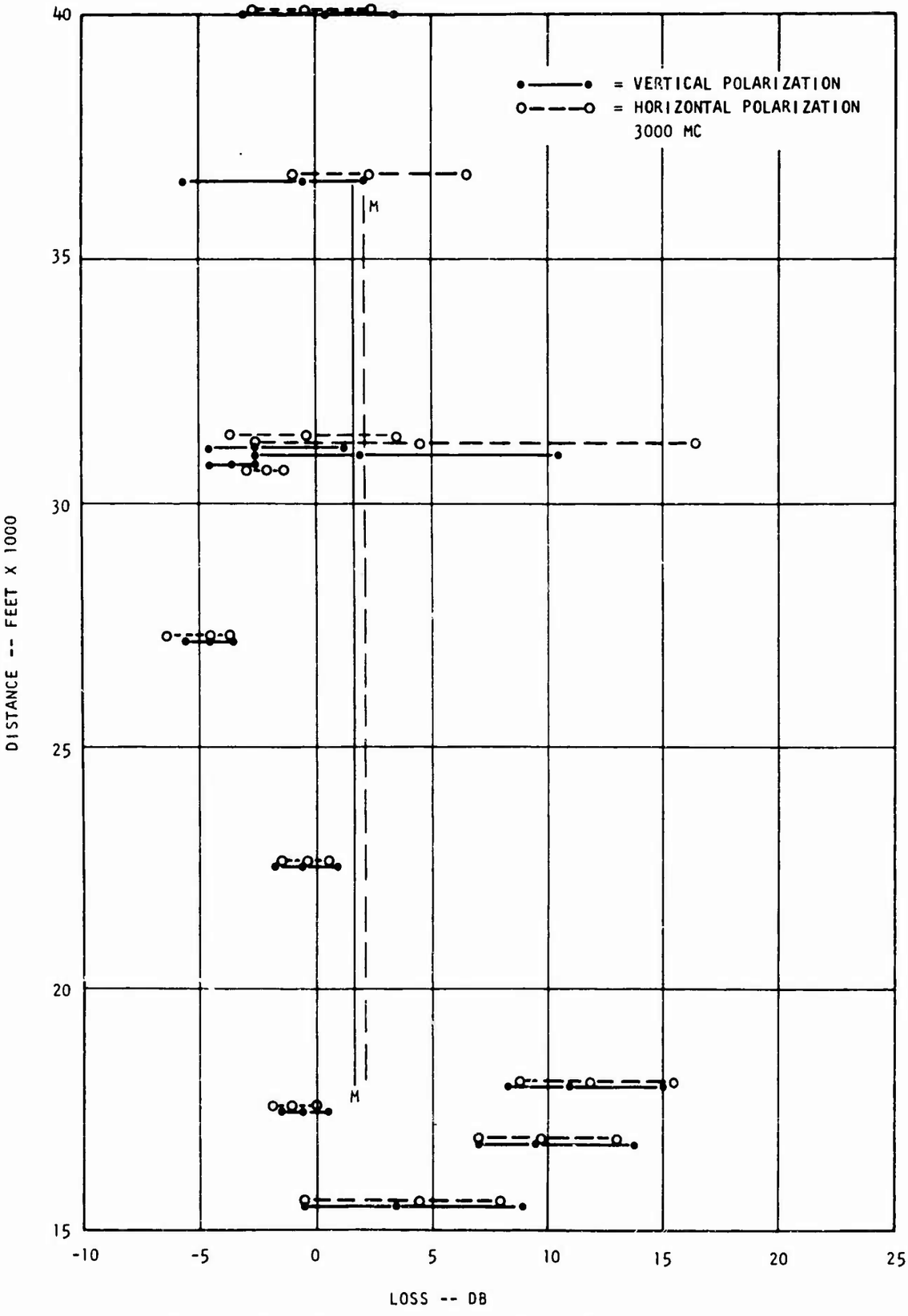

Figure 13e. Propagation Loss Plots, Loss at 3000 Mc.

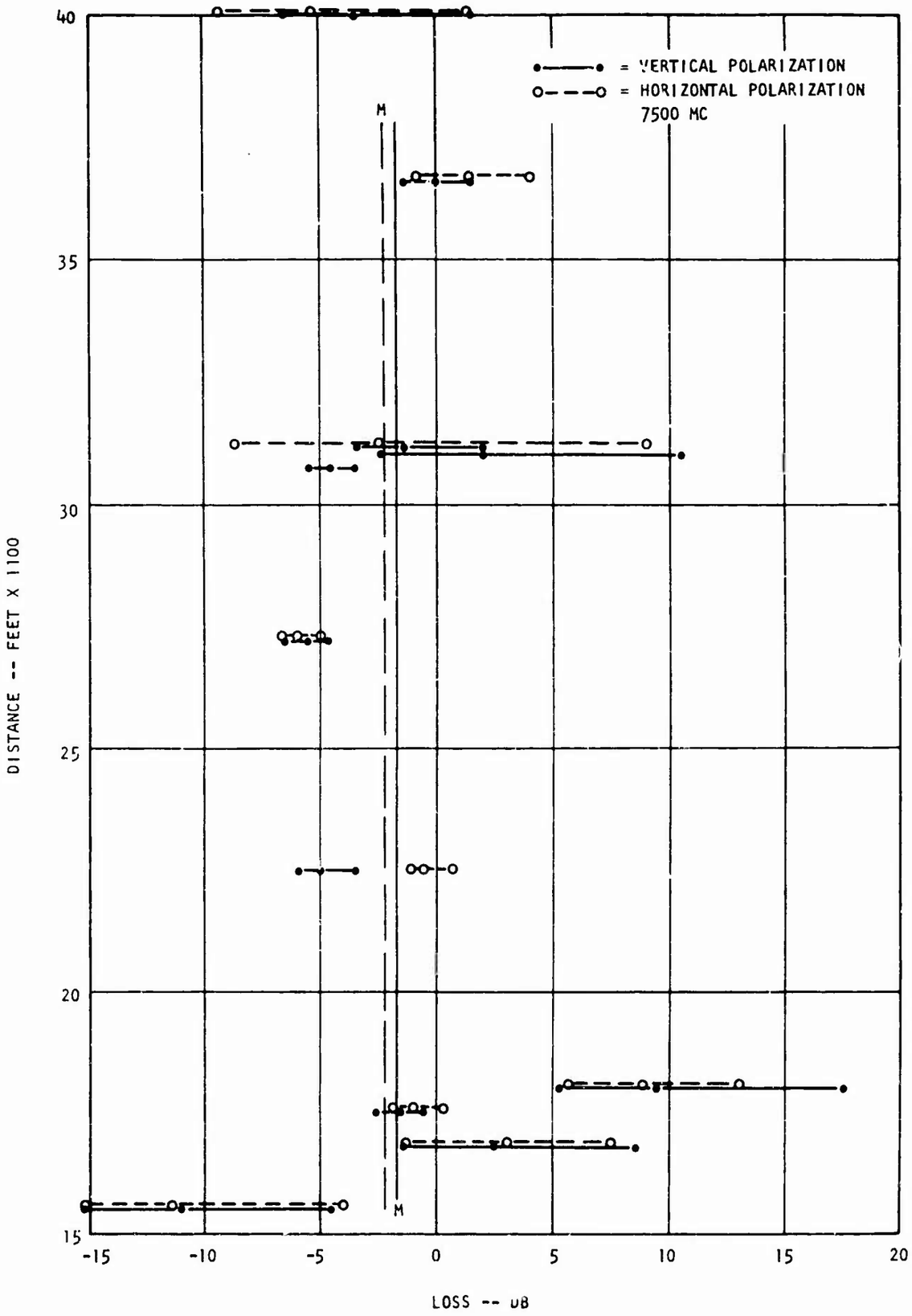

Figure 13f. Propagation Loss Plots, Loss at 7500 Mc.

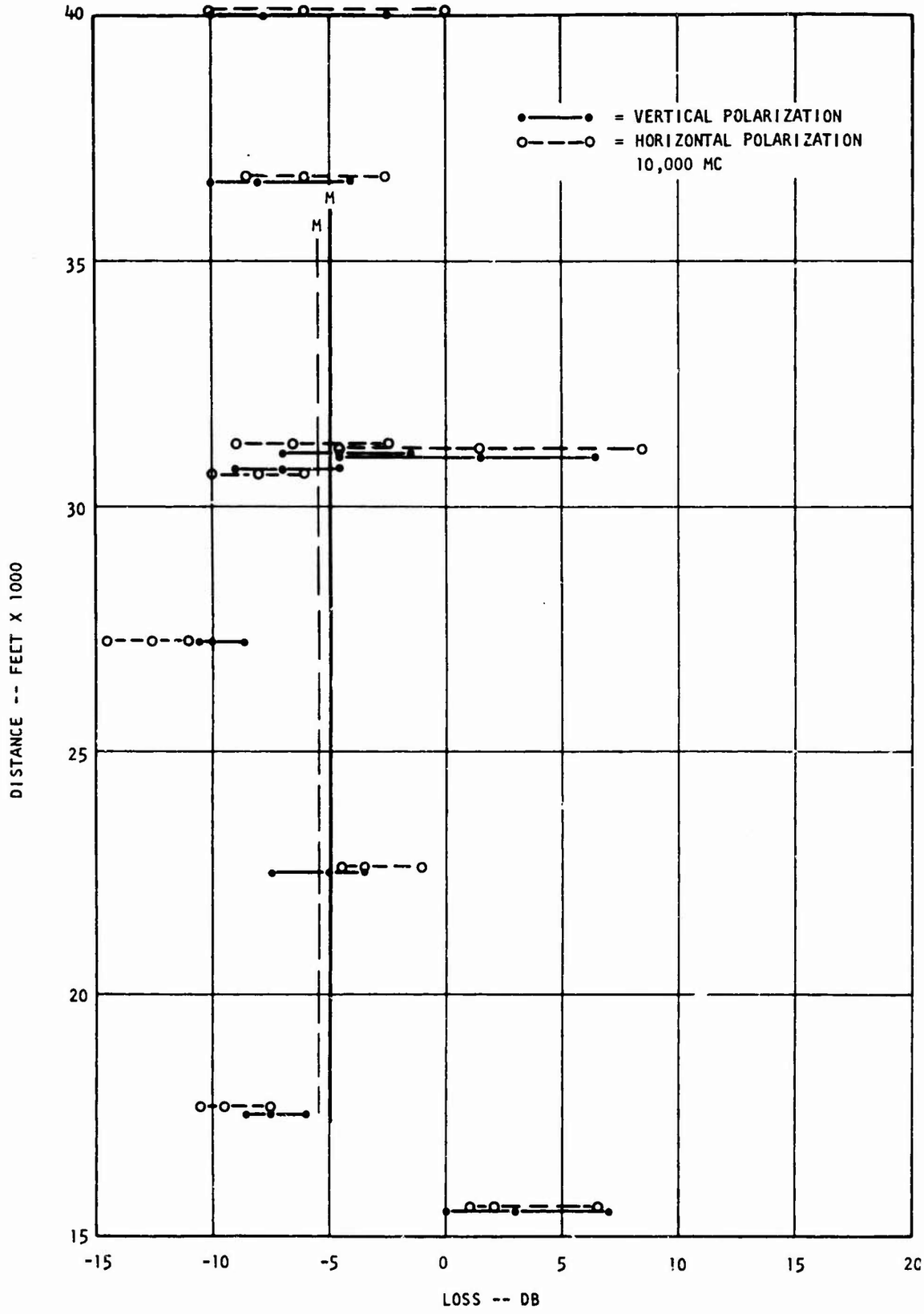

Figure 13g. Propagation Loss Plots, Loss at 10,000 Mc.

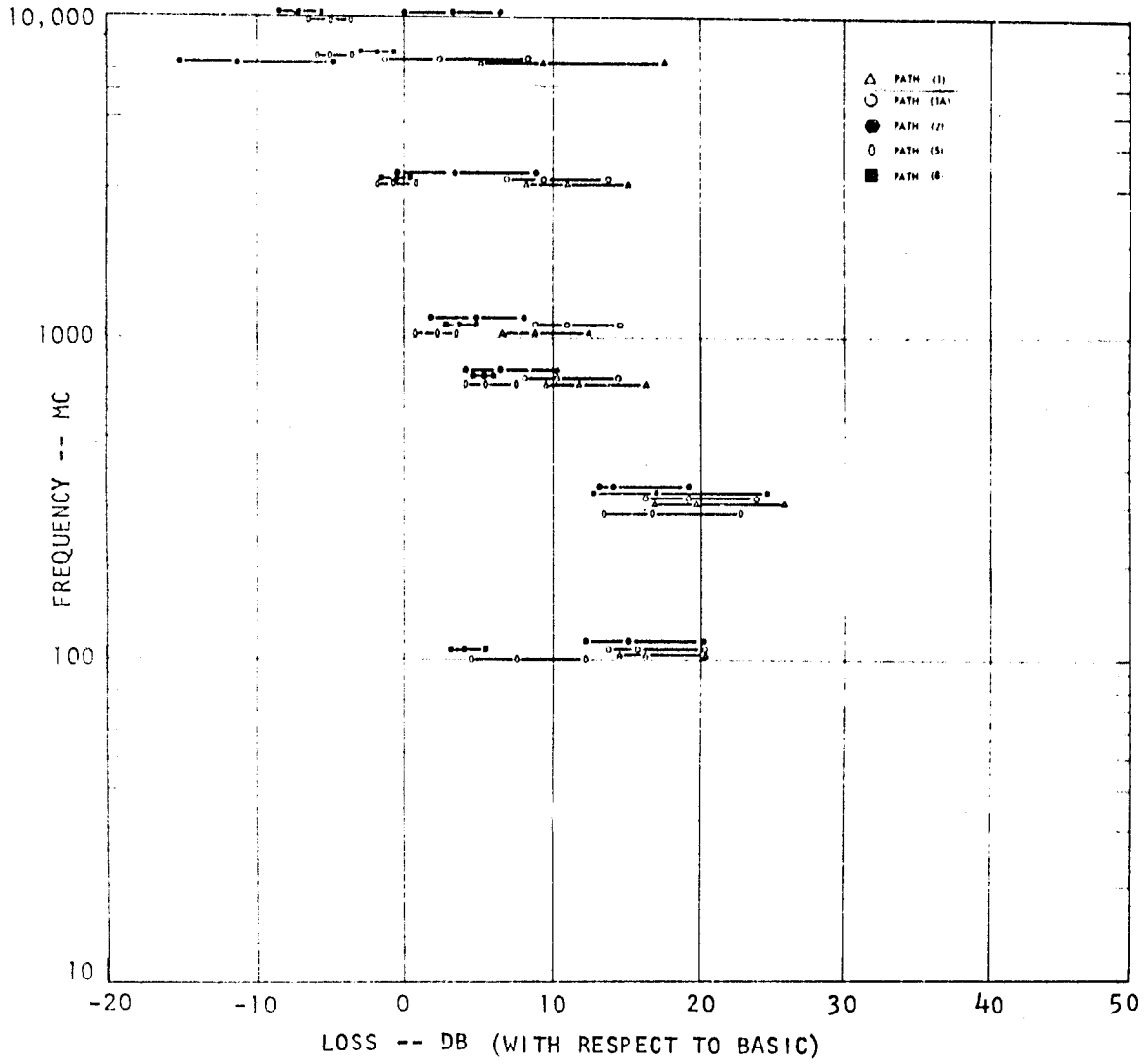

Figure 14a. Path Loss as a Function of Frequency for Each of the Paths, Vertical Polarization, Paths 1, 1A, 2, 5, and 8.

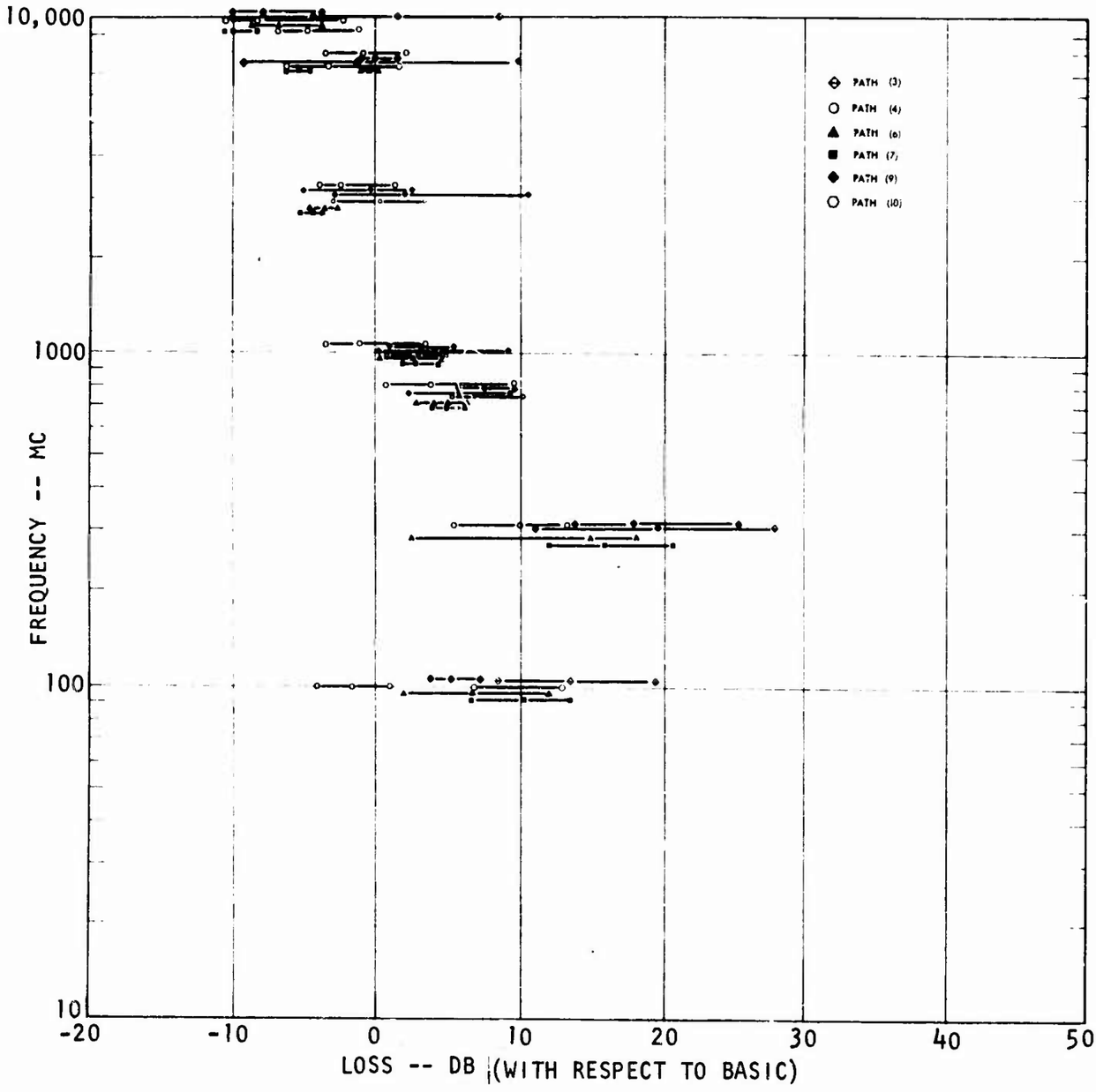

Figure 14b. Path Loss as a Function of Frequency for Each of the Paths, Vertical Polarization, Paths 3, 4, 6, 7, 9, and 10.

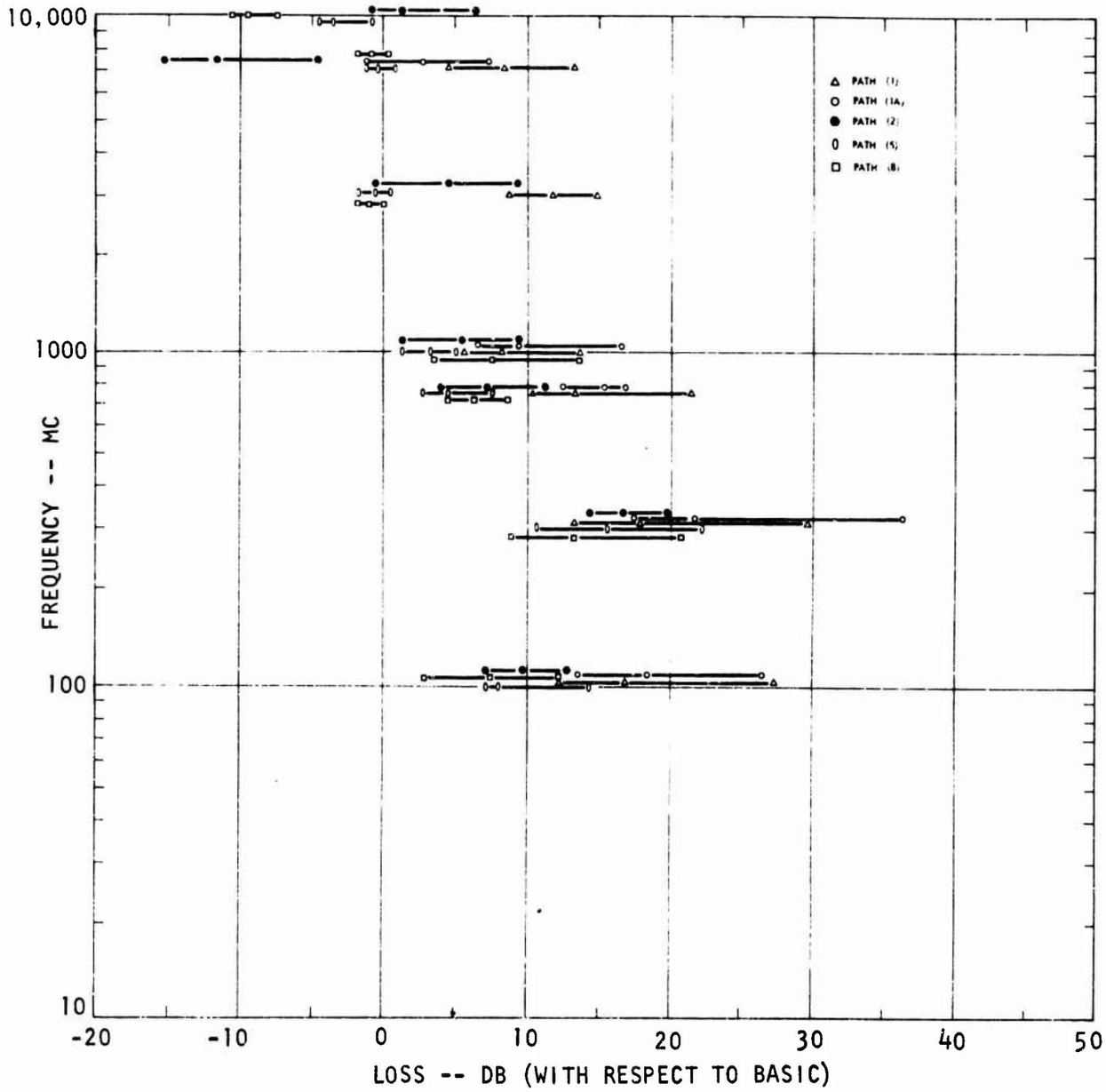

Figure 15a. Path Loss as a Function of Frequency for Each of the Paths, Horizontal Polarization, Paths 1, 1A, 2, 5, and 8.

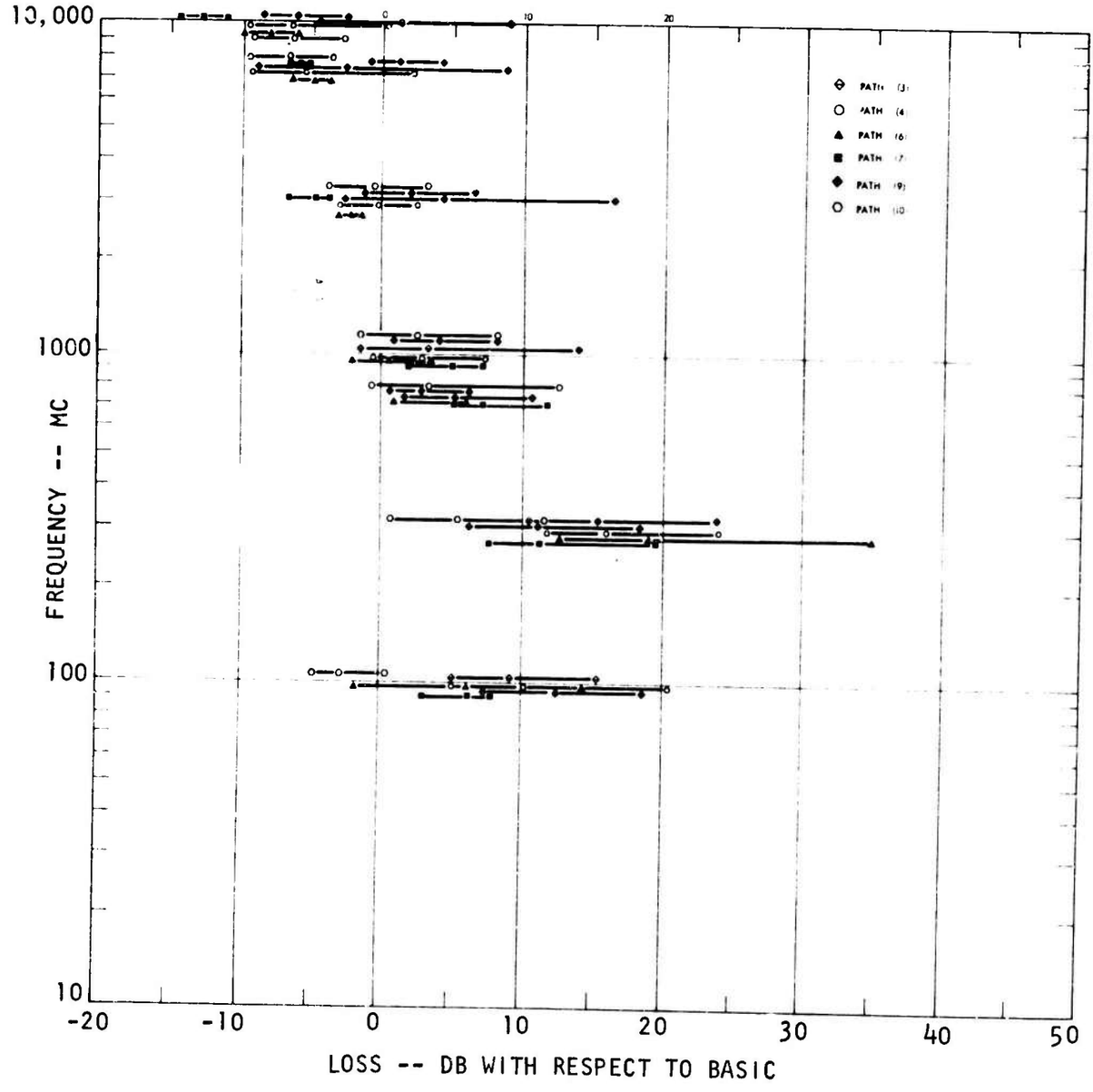

Figure 15b. Path Loss as a Function of Frequency for Each of the Paths, Horizontal Polarization, Paths 3, 4, 6, 7, 9, and 10.

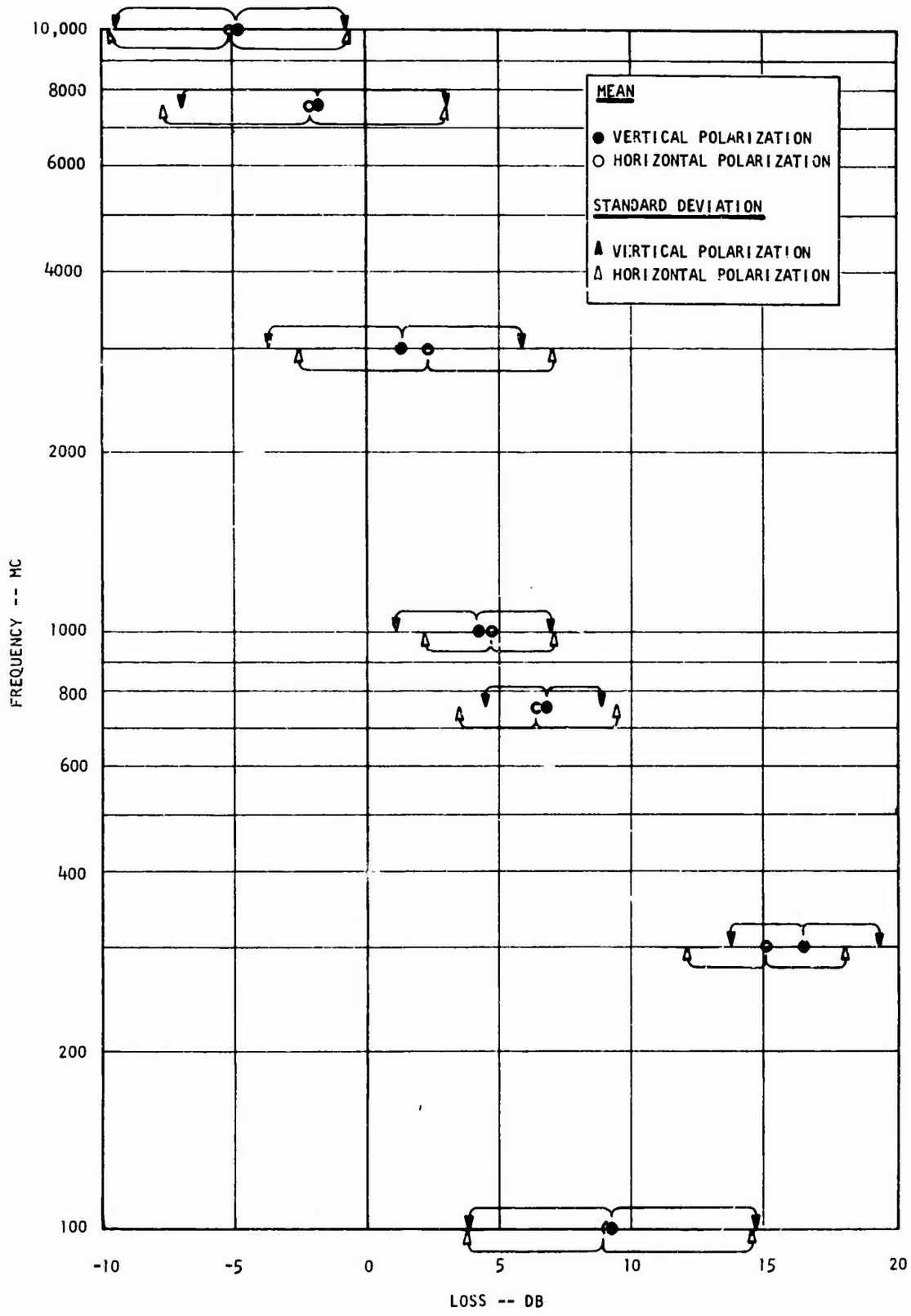

Figure 16. Mean and Standard Deviation for the Average Loss for All Paths.

Section 7

EXPERIMENTAL RESULTS AND MODEL CHANGES

The experiments have shown that, independent of the kind of path, the following effects generally occur.

a. Specular reflection is present at all frequencies, and it predominates at low frequencies.

b. The specular and diffuse reflection coefficients decrease with increasing frequency.

c. For a given frequency, LOS propagation loss with respect to effective free-space loss is independent of path length.

d. For frequencies above 350 Mc, propagation loss above effective free-space loss decreases with increasing frequency.

The original model contained no provision for incorporating the effects of specular reflection, nor was the diffuse reflection coefficient assumed to have a frequency dependence. Moreover, since the number of scatterers was determined by geometrical means and was independent of frequency, no way of indicating a decrease in average loss as the frequency increases was inherent in the model. Suitable modifications must therefore be made in the model to incorporate the four above effects.

7.1 Reflection Coefficient.

7.1.1 Specular Reflection at 500 Mc and Above.

At the higher frequencies (3000, 7500, and 10,000 Mc), the values of the specular reflection coefficient tend to approach 0.20. Although a full period could not always be examined at 750 and 1000 Mc, it appears that ρ_s does not greatly exceed 0.35. This can be seen from the fact that, of the portions of periods observed at these frequencies for all the paths, the variation of the specular component rarely exceeds 6 or 7 db. The following values are used for ρ_s, independent of path and polarization.

7.1.1 --Continued

Frequency (Mc)	ρ_s
500 - 800	0.35
800 - 2000	0.27
2000 - 20,000	0.20

7.1.2 Specular Reflection Below 500 Mc.

Values of ρ_s will be expected to range from 0.50 to approximately 1.00 at these frequencies, depending on terrain and angle of incidence. Sherwood and Ginzton's curves[6] for harrowed field (slight vegetation) and rolling field (heavy vegetation) are used to determine the magnitude of the reflection coefficient.

7.1.3 Diffuse Reflection at 500 Mc and Above.

The diffuse reflection coefficient, containing the varying parts of diffuse and specular components, both assumed to be Rayleigh distributed, are assigned values corresponding to the experimental results; ρ_d takes on the following values, independent of path and polarization.

Frequency (Mc)	ρ_d
500 - 800	0.37
800 - 2000	0.30
2000 - 20,000	0.23

7.1.4 Diffuse Reflection Below 500 Mc.

At frequencies below 500 Mc, it is assumed that the diffuse component is negligible.

7.2 Variation of the Number of Scatterers with Frequency Above 500 Mc Only.

The measurements have indicated that the mean loss, with respect to free-space loss, decreases with increasing frequency. Since the diffuse component is taken

7.2 --Continued

as Rayleigh distributed, the total diffuse scattered power, normalized to the direct wave, increases with frequency. The diffuse reflection coefficient observed in the experiments tended to decrease with frequency and, therefore, retention of the basic model necessitates an increase in the number of scatterers as the frequency increases. Assume the requirements for a scatterer are (1) a surface of dimension, γ such that $\gamma >> \lambda$ and (2) a linear relation between the scatterer size and the wavelength (e.g., $\gamma = 100\,\lambda$). If a particular shape for a scatter is selected, much more complicated expressions can be shown to exist.[10] However, little would be gained by incorporating such complexity into the model, for the true "shape" of a scatterer will almost always be unknown.

The criterion for the number of scatterers along a reflecting surface will be taken as one scatterer per 100 λ of surface extent for a given segment.

Section 8

MODEL FOR DETERMINING LOS PROPAGATION LOSS

8.1 Below 500 Mc (Specular Reflection Predominant Mode*).

The following procedure is used to determine LOS propagation loss below 500 Mc.

a. Compute the amplitude of the field, E_o, at the receiving antenna due to the direct wave.

b. Determine all segments of the surface capable of reflecting directly from transmitting antenna to receiving antenna. Maximum segment size is 125 meters.

c. Compute the angle of incidence to each segment, such that the angle of incidence equals the angle of reflection.

d. Determine the reflection coefficient as a function of the angle of incidence, polarization, and terrain cover, from the empirical curves of Sherwood and Ginzton.[6]

e. Determine the amplitude of the resultant field at the receiver, E, by vectorially adding the direct wave and the reflected waves:

$$E = \left| E_o + \sum_{k=1}^{m} \rho_{sk} E_o e^{j\varphi_k} \right| , \qquad (18)$$

where ρ_{sk} is the magnitude of the specular reflection coefficient from the k^{th} segment.

*The deep nulls, which must be expected when specular reflection predominates, cannot be incorporated into the model. Variations in magnitude of up to 20 db about the calculated value must be expected to occasionally arise.

8.1 --Continued

f. Compute propagation loss.

$$L = L_{eff} - 20 \log_{10} \frac{E}{E_o} \tag{19}$$

$$= L_{eff} - 20 \log_{10}\left(\frac{1}{E_o} \left| E_o + \sum_k \rho_{sk} E_o e^{j\varphi_k} \right| \right) \tag{20}$$

$$L = 36.6 + 20 \log_{10} d_{mi} + 20 \log_{10} f_{mc} - G_T - G_R + D$$

$$- 20 \log_{10}\left(\frac{1}{E_o} \left| E_o + \sum_k \rho_{sk} E_o e^{j\varphi_k} \right| \right). \tag{21}$$

8.2 Above 500 Mc (Specular and Diffuse Reflection Considered).

To determine LOS propagation loss above 500 Mc, employ the following procedure.

a. Compute the amplitude of the field, E_o, at the receiving antenna due to the direct wave.

b. Determine all segments of the surface capable of reflecting directly from transmitting antenna to receiving antenna. Maximum (specular) segment size is 125 meters.

c. Select from the experimental curves of Sherwood and Ginzton, the curve with vegetation cover most similar to the surface under consideration.

d. Determine the relative amplitude of the reflection coefficient for each segment by normalizing to that segment with the largest reflection coefficient.

8.2 --Continued

e. Sum the reflected waves vectorially to determine the phase, φ, of the resultant specular wave. This is the phase difference between the direct wave and the resultant specular wave.

f. Select the appropriate value for the magnitude of the specular reflection coefficient from paragraph 7.1.1, giving values of ρ_s versus frequency.

g. Obtain the amplitude of the resultant specular component, E, by adding (vectorially) the direct wave, E_c, and the resultant scattered wave, $\rho_s E_o e^{j\varphi}$; that is,

$$E = \left| E_o + \rho_s E_o e^{j\varphi} \right| . \tag{22}$$

h. Select the appropriate value for the diffuse reflection coefficient from paragraph 7.1.3, giving ρ_d versus frequency.

i. Determine the number of scatterers, σ, for each of the (diffuse) reflecting segments from

$$\sigma = \frac{L}{100\,\lambda} , \tag{23}$$

where L is the length of the illuminated segment.

j. Calculate the total diffuse scattered power, E_1^2, from

$$E_1^2 = \sum_{k=1}^{m} \left[\sum_{j=1}^{\sigma_k} \left(\rho_d E_o \right)_j^2 \right]_k . \tag{24}$$

8.2 --Continued

k. Compute the distribution of the amplitude of the field at the receiver, R(P), as in the original model, but use the Equation (24) value for E_1^2 and change R from $R = 20 \log_{10} \frac{E}{E_o}$ to

$$R = 20 \log_{10} \frac{E}{\left| E_o + \rho_s E_o e^{j\varphi} \right|} . \tag{25}$$

l. Subtract R(P) from L'^{*}_{eff} to find the LOS propagation loss, L(P).

$$L(P) = L'_{eff} - R(P)$$

$$L(P) = 36.6 + 20 \log_{10} d_{mi} + 20 \log_{10} f_{mc} - G_T - G_R + D + 20 \log_{10} \frac{E_o}{\left| E_o + \rho_s E_o e^{j\varphi} \right|} - R(P) \tag{26}$$

---

* $L = 20 \log \frac{E_T}{E}$

where

E_T = amplitude of the transmitted field

E = amplitude of the received field.

Then

$$L = 20 \log \frac{E_T}{E} \cdot \frac{E_o}{E_o} = 20 \log \frac{E_T}{E_o} + 20 \log \frac{E_o}{E}$$

$$= 20 \log \frac{E_T}{E_o} + 20 \log \frac{E_o}{E} \cdot \frac{\left| E_o + \rho_s E_o e^{j\varphi} \right|}{\left| E_o + \rho_s E_o e^{j\varphi} \right|}$$

$$= 20 \log \frac{E_T}{E_o} + 20 \log \frac{E_o}{\left| E_o + \rho_s E_o e^{j\varphi} \right|} - 20 \log \frac{E}{\left| E_o + \rho_s E_o e^{j\varphi} \right|}$$

8.2 --Continued

$$L = L_{eff} + 20 \log \frac{E_o}{|E_o + \rho_s E_o e^{j\varphi}|} - R$$

$$= L'_{eff} - R.$$

Section 9

CONCLUSIONS AND RECOMMENDATIONS

An extensive series of experiments have been conducted to gain more information on LOS scattering so the model might more accurately describe this phenomenon. A number of paths of varying irregularity, roughness, and vegetation cover have been studied to determine the effects of these parameters on path loss and magnitude of reflection coefficient. Frequencies considered have ranged from 100 Mc to 10,000 Mc, with both horizontal and vertical polarization employed.

The experiments have shown (1) that specular reflection must be incorporated into the model at all frequencies and (2) that the magnitude of the specular reflection coefficient and the diffuse reflection coefficient exhibit frequency dependence. At frequencies above 500 Mc, this frequency variation results in magnitude ranges of approximately 0.20 to 0.40 for both reflection coefficients. For frequencies below 500 Mc, the specular reflection coefficient may range from as low as 0.20 to approximately unity.

The experiments have also indicated that propagation loss above effective free-space loss is independent of path length and decreases with increasing frequency above 300 Mc. For most measurements made at frequencies above 3000 Mc, the average loss, irrespective of path, was less than that predicted for effective free-space propagation. The causes of the excessive loss at 300 Mc, again independent of path, should be investigated further.

The line-of-sight (LOS) propagation model was modified to more accurately reflect the effects of the two scattering modes, specular and diffuse, in determining loss over rough and irregular terrain where only segments of the surface are illuminated.

At frequencies below 300 Mc, specular reflection is the predominant mode of scattering, and geometrical means are used to predict signal strength at the receiver. The occurrence of fades, resulting in variation of 10 to 20 db, cannot be predicted with this model and will require additional study.

9. --Continued.

In the frequency range 750 to 20,000 Mc, specular and diffuse reflections are present, and a combination of geometrical and statistical methods are used to predict the field at the receiver. The magnitudes of the fades are much less at these frequencies, and consequently, the absence of a mechanism to predict the fading rate does not limit the use of the model.

The frequency range 300 to 750 Mc, unexplored in the present experimental program, provides the greatest uncertainty in the model. The midway point in this region was arbitrarily chosen as the changeover point from one mode to the other. It is recommended that an extensive study of reflection at these frequencies take place in future experimental programs.

Section 10

REFERENCES

1. Elliott, D., "A Computer Model for the Simulation of Tactical Signal Environments," Technical Memorandum EDL-M768, Sylvania Electronic Defense Laboratories; 21 December 1964.

2. Ament, W. S , "Toward a Theory of Reflection by a Rough Surface," Proc. IRE, vol. 41, pp. 142-146; 1953.

3. Rice, S. O. , "Reflection of Electromagnetic Waves from Slightly Rough Surfaces," Comm. Pure and Applied Math, vol. 4, pp. 351-378; 1951.

4. Beckmann, P. , "On the Problem of the Scattering of Very Short Waves from Rough Surfaces," (in Czech.), Slab Opr. Obz. , vol. 14, pp. 302-309; 1953.

5. Elliott, D. and Smith J. , "Automated Signal Environment Model: Revised Capabilities," Technical Memorandum EDL-M879, Sylvania Electronic Defense Laboratories; 22 November 1965.

6. Sherwood, E. M. and Ginzton, E. L. , "Reflection Coefficient of an Irregular Terrain at 10 cm," Proc. IRE, vol. 43, p. 877; 1955.

7. Rice, S. O. , "Mathematical Analysis of Random Noise," Bell Syst. Tech. Jour. , vol. 23, pp. 282-332; 1944.

8. Norton, K. A. , Vogler, L. E. , et al. , "The Probability Distribution of the Amplitude of a Constant Vector Plus a Rayleigh-Distributed Vector," Proc. IRE, vol. 43, pp. 1354-1361; 1955.

9. Beckmann, P. and Spezzichino, A. , "The Scattering of Electromagnetic Waves from Rough Surfaces," MacMillan; 1963. (pp. 305-306)

10. Twersky, V. , "On Scattering and Reflection of Electromagnetic Waves in Rough Surfaces," IRE Trans. on Antennas and Propagation, vol. 5, no. 1, pp. 81-89; January 1957.

UNCLASSIFIED
Security Classification

DOCUMENT CONTROL DATA - R&D
(Security classification of title, body of abstract and indexing annotation must be entered when the overall report is classified)

1 ORIGINATING ACTIVITY (Corporate author) Sylvania Electronic Defense Laboratories P. O. Box 205 Mountain View, California	2a. REPORT SECURITY CLASSIFICATION UNCLASSIFIED 2b. GROUP

3 REPORT TITLE
LINE-OF-SIGHT PROPAGATION EXPERIMENTATION AND MODELING FOR PARTIALLY ILLUMINATED TERRAIN

4 DESCRIPTIVE NOTES (Type of report and inclusive dates)
Technical Memorandum

5 AUTHOR(S) (Last name, first name, initial)
Harry N. Gitterman
Samuel N. Watkins

6. REPORT DATE	7a. TOTAL NO. OF PAGES	7b. NO. OF REFS
1 November 1965	76	10

8a. CONTRACT OR GRANT NO. DA 28-043 AMC-00379(E) b. PROJECT NO. c. d.	9a. ORIGINATOR'S REPORT NUMBER(S) EDL-M878 9b. OTHER REPORT NO(S) (Any other numbers that may be assigned this report)

10. AVAILABILITY/LIMITATION NOTICES
Distribution of this document is unlimited.

11. SUPPLEMENTARY NOTES	12. SPONSORING MILITARY ACTIVITY
	U.S. Army Electronics Command Fort Monmouth, New Jersey

13. ABSTRACT

A series of experiments was conducted to evaluate a model that predicts line-of-sight (LOS) propagation loss over partially illuminated terrain. Height-gain measurements were made at the receiver for a number of paths of varying irregularity, roughness, and vegetation cover. The measurements indicate that two regions must be recognized: the first, below 500 Mc, where specular effects are predominant and the specular reflection coefficient varies from approximately 0.20 to unity; and the second, above 500 Mc, where both the specular and the diffuse components must be considered and where both the specular and the diffuse reflection coefficients generally range from 0.20 to 0.40. Appropriate changes have been made in the original LOS model to reflect more accurately the propagation effects in these two regions over the frequency range of interest, 40 Mc to 20 Gc.

DD FORM 1 JAN 64 1473

UNCLASSIFIED
Security Classification

UNCLASSIFIED

Security Classification

14. KEY WORDS	LINK A		LINK B		LINK C		KEY WORDS (Cont)	LINK A		LINK B		LINK C	
	ROLE	WT	ROLE	WT	ROLE	WT		ROLE	WT	ROLE	WT	ROLE	WT
*Line													
*Sight													
*Propagation													
*Experimentation													
*Modeling													
*Partially													
*Illuminated													
*Terrain													
Reflection													
Coefficients													
Specular													
Diffuse													
Loss													
500MC													
40MC - 20GC													
Variation													
Number													
Scatterers													
Frequency													
Predicts													
Mode													
Height													
Gain													
Receiver													
Path													
Measurements													
Irregularity													
Roughness													
Vegetation													
Cover													
Transmitter													
Signal													
Environment													
Angle													
Incident													
Grazing													
Function													
Scattered													
Power													
Phase													
Coherence													
Radiation													
Free													
Space													
Amplitude													
Polarity													
Horizontal													
Vertical													
Rayleigh													
Probability													
Distribution													

UNCLASSIFIED